

# Brownian motion in complex fluids: venerable field and frontier of modern physics<sup>†</sup>

A. Vizcarra-Rendón, M. Medina-Noyola\*,

H. Ruiz-Estrada and J.L. Arauz-Lara

*Departamento de Física, Centro de Investigación y de Estudios Avanzados,  
Instituto Politécnico Nacional, Apartado postal 14-740, 07000 México, D.F.*

(Recibido el 5 de junio de 1989; aceptado el 26 de julio de 1989)

**Abstract.** This paper reviews the current status of our understanding of tracer-diffusion phenomena in colloidal suspensions. This is the most direct observation of the Brownian motion executed by labelled Brownian particles interacting with the rest of colloidal particles in a suspension. The fundamental description of this phenomenon constitutes today one of the most relevant problems in the process of understanding the dynamic properties of this important class of complex fluids, from the experimental and theoretical perspective of physical research. This paper describes the recent developments in the extension of the classical theory of Brownian motion and its application to the description of the effects of direct and hydrodynamic interactions among colloidal particles. As a result, a coherent picture has emerged in which the agreement between theory and experiment has the degree of qualitative and quantitative accuracy expected from more mature fields of physics. The moral of the paper is that the use of well established concepts of statistical physics, assisted by modern experimental techniques, are contributing to transform complex fluids into a more amiable class of materials from the point of view of the physicist.

PACS: 05.40.+j; 05.70.Ln; 47.15.Pn

## 1. Introduction

The study of complex fluids constitutes today one of the most relevant and novel fields of research in materials science and engineering. For complex fluids we refer to fluid systems, whose most important properties (thermodynamic, transport, rheological, etc.) derive from a well-defined spatial and temporal structure at the supramolecular level, *i.e.*, intermediate between the molecular and the macroscopic scale [1-4]. Examples of such materials are colloidal dispersions, or sols (formed by finely dispersed solids in liquids), macromolecular, polyelectrolyte, and micellar

---

<sup>†</sup>Some aspects of this paper were presented in a plenary lecture delivered by the second author at the XXXI Annual Meeting of the Mexican Physical Society, in Monterrey, Nuevo León, México. (October, 1988).

\*Also at Departamento de Ciencias Básicas, Universidad Autónoma Metropolitana, Unidad Azcapotzalco, México, D.F.

solutions, microemulsions, etc. In these materials, a large number of different microstructures can be formed, such as colloidal liquids and colloidal crystals, fractal aggregates, microdroplets, vesicles, bicontinuous phases, filamentary and porous structures, etc. Many industrial and commercial products, both natural and artificial, involve in their processing, or in their final form, this type of materials. Among such products, one could mention foods, like milk, many pharmaceuticals, cosmetics, paints, petrochemicals, fertilizers, and polymeric and plastic materials.

In spite of their apparent diversity, there is a less apparent but important uniformity, among the various classes of complex fluids, namely, in the general approaches employed in their experimental and theoretical study. This is more obvious when we consider the physical and chemical methods employed to probe their supramolecular structure and dynamics [1–5]. Thus, physical techniques such as static and dynamic light scattering, small-angle x-ray and neutron scattering, etc., have been devised or adapted to study each particular type of complex fluids. The attitude, however, is always the same, namely, one expects to explain the less detailed, macroscopic behaviour of these materials, in terms of effective interaction forces acting at the supramolecular level, and of the microstructural properties that such interactions induce.

On the other hand, the study of Brownian motion, as pioneered by Einstein [6], Smoluchowsky [7] and Langevin [8], among others, constitutes one of the most prolific contributions to science. Thus, a large number of theories describing fluctuations and random properties of systems constitute today important and active fields of contemporary science, whose lineage may be traced back to the work of those men. Among such living and healthy heirs of the classical theory of Brownian motion, one could mention the mathematical theory of stochastic processes, the irreversible-thermodynamic theory of fluctuations with its myriad of applications in physics and chemistry, and the theory of noise and its applications in engineering and science. In particular, the theoretical understanding of the dynamic properties of complex fluids constitutes another concrete example of an active field of statistical physics, whose genealogy traces back to the classical theory of Brownian motion. Thus, generalizations of the classical theory to describe the random motion of random surfaces in a bicontinuous microemulsion, the Brownian motion of a particle within the filamentary matrix of a gel, or the irreversible trajectories leading to the formation of fractal aggregates in an unstable colloid, could be typical examples of the questions awaiting the development and generalization of the theory of Brownian motion, aimed at understanding complex fluids from a fundamental perspective.

One of the most common structures formed by complex fluids is that of a suspension, *i.e.*, a set of well-defined entities, generically termed macroparticles (such as macromolecules, micelles, microdroplets, small pieces of solid material, etc.), suspended in a continuous fluid phase (the solvent). The Brownian motion of each macroparticle in a concentrated suspension is, of course, highly correlated with the motion of many other particles with which it collides and interacts by means of direct and hydrodynamic forces [5–9]. We call direct interactions the conservative forces between particles, such as electrostatic, van der Waals, hard-sphere, etc., which may be described by an interaction potential function. Direct forces are responsible for a

local average ordering of the macroparticles around any one of them considered fixed. The function describing this local order represents the microstructural information of the suspension, and is determined, at thermodynamic equilibrium, solely by the direct interaction forces.

Hydrodynamic interactions, on the other hand, are the velocity-dependent, non-conservative forces that each macroparticle experiences, due to the local velocity field of the solvent, constantly perturbed by the motion of all the other particles [10,11]. Although these forces do not affect any equilibrium (structural or thermodynamic) property, their effects show quite dramatically in the transport properties of concentrated suspensions.

The fundamental understanding of suspensions involves the establishing of a precise relationship among the concept of forces between macroparticles, supramolecular microstructure, and thermodynamic and transport properties. Clearly, the study of the Brownian motion in concentrated suspensions constitutes an important aspect of this general program, and it is the main purpose of this paper to review the current status of our understanding of a particular class or phenomena, namely, of the self-diffusion properties of suspensions. As we shall see, a coherent and precise description of the main effects affecting the Brownian motion in concentrated suspensions has emerged rather recently, at least when dealing with clean and well-defined model systems, both experimentally and theoretically. We would like to conclude, as a consequence, that in this parcel of the study of complex fluids, physics has provided the degree of qualitative and quantitative understanding which is common to other mature areas of physical research, and that those other aspects of complex fluids which remain to be understood, constitutes a genuine frontier of modern physics.

In most of this work, we shall have in mind suspensions of spherical macroparticles of a single type (*i.e.*, monodisperse). We shall first discuss the properties of dilute suspensions of highly charged colloidal particles in water. In this case, the effective pair potential  $u(r)$  describing the electrostatic repulsive forces between macroparticles may be represented by a screened Coulomb potential. This is a rather long-ranged potential compared to the hard-sphere repulsion associated to the actual physical diameter  $\sigma$  of the particles. Thus, although the suspension may be highly dilute with respect to the volume fraction occupied by the macroparticles, the electrostatic forces strongly correlate the positions and the motion of all the suspended particles. For such systems, hydrodynamic interactions are negligible. Furthermore, their static structural properties are by now well understood, and the agreement between theory and experiment may be said to be satisfactory, as it is discussed and illustrated in section 2. Thus, these systems will serve to illustrate the approach employed in the study of complex fluids.

With the structural problem assumed understood, one may proceed to the discussion of the dynamic properties. In section 3 we discuss and illustrate the difference between collective- and self-diffusion phenomena. Self-diffusion is the direct experimental observation of the Brownian motion of individual macroparticles, and the rest of the paper centers on that subject. Section 4 provides a simple, intuitive picture of one of the main features of Brownian motion in concentrated suspension,

namely, the existence of well-separated time-scales defined by the effects of the direct interactions. In section 5 we illustrate the current status of our understanding of self-diffusion experiments performed in highly correlated but hydrodynamically dilute suspensions, in terms of two well-established theories.

Unfortunately, the consideration of hydrodynamic interactions demand extensions of those two theoretical approaches, which at least from a practical point of view, seem exceedingly complicated. Thus, in section 6 we describe a third theoretical formalism to the description of self-diffusion phenomena based on general principles of the linear irreversible thermodynamic theory of fluctuations [12,13]. Its application to the theory of Brownian motion in highly correlated suspensions constitutes a simple example of the idea of contraction of the description, also explained and illustrated in that section. This results, in our case, in a generalized Langevin equation for a tracer Brownian particle that diffuses in a suspension of many other strongly correlated colloidal particles (Eq. (18)). Although the general results thus derived lead in a particular case, to one of the theories discussed in section 4, it lends itself to rather simple extensions to incorporate the effects of hydrodynamic interactions. Section 6 contains a rather detailed and elementary derivation of the main results of this theory, as well as the description of a more formal derivation. A more pragmatic reader may accept the main results of the theory, namely, Eqs. (36) and (37), and proceed to their applications in the subsequent sections.

Section 7 describes the application of this theory to the interpretation of self-diffusion experiments in concentrated hard-sphere like suspensions. These systems are the opposite extreme from the electrostatically correlated systems discussed in section 4, in the sense that the direct interactions are hard-sphere (and hence, short-ranged) rather than screened (but much longer ranged) coulombic interactions, and in that hydrodynamic interactions constitute a most important feature, affecting self-diffusion in all time-regimes.

Section 8 addresses a rather different effect. Considering *charged* Brownian particles *at infinite dilution*, another source of friction must be considered, namely, the friction on the particle due to its interaction with the counterions and the other small ions of the supporting solution. This is a rather small effect compared to that of the direct interactions with other Brownian particles, but its features can be clearly observed experimentally in the limit of extremely dilute suspensions. In section 8, we describe the application of the same general results of section 6 to this problem, with the intention to illustrate the power of the method. Finally, section 9 summarizes briefly the main aspects of this paper, and discusses the perspective for progress in this field.

## 2. Static structure of suspensions

In the study of suspensions, the very first problem is the determination of the local average microstructure around each suspended particle. In comparison, for crystalline materials, this microstructure may be determined directly from the observation of their Bragg diffraction patterns. Thus, the physics of crystalline solids

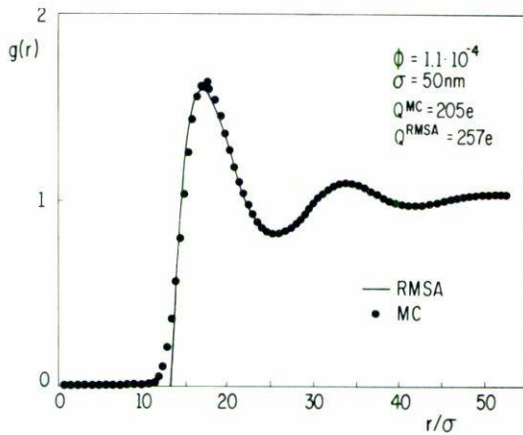


FIGURE 1. Radial distribution function of a salt-free aqueous suspension at room temperature of highly charged polystyrene particles of charge  $Q$ , hard-sphere diameter  $\sigma$ , number concentration  $n$ , and volume fraction  $\phi (= \pi n \sigma^3 / 6)$ , which interact through the DLVO potential in Eq. (1) with a screening length  $\kappa^{-1} = 11.49\sigma$ . The dots are computer simulation (Monte Carlo) data, and the solid line is a theoretical calculation based on the rescaled mean spherical approximation. The corresponding static structure factors fit the experimental results in a manner illustrated in Fig. 2 for a similar sample, using  $Q$  as the only fitting parameter. (Figure reproduced from ref. [18]).

has focussed traditionally on other phenomena, such as the electronic properties of those materials. A similarly privileged condition is not shared by complex fluids, and not even by ordinary (atomic and molecular) liquids. Here, the ordered, long-ranged periodic structure of a solid is replaced by an average, short-ranged, local structure, whose determination is the very first relevant and fundamental task in their study. The quantity containing this microstructural information of a liquid is the so-called radial distribution function  $g(r)$ . This function, times the bulk number density  $n$ , gives the average local density of particles around a given particle fixed at  $\mathbf{r} = 0$ . It vanishes in a region centered around  $\mathbf{r} = 0$ , since the very presence of the fixed particle excludes other particles, from such a region. At long distances,  $g(r) \rightarrow 1$ , indicating the loss of the order induced by the central particle. The general features of  $g(r)$  are illustrated in Fig. 1, where the radial distribution function of a suspension of highly charged polystyrene spheres in water is plotted. As it happens, the development of the theory of simple liquids during the last three decades generated a wealth of theoretical and experimental techniques to determine the structural properties of liquids [14]. During the present decade, the study of suspensions has benefitted directly from such progress. This is due to the fortunate analogy between a colloidal suspension and a simple liquid [15], in which the colloidal particles play the role of the molecules in an ordinary liquid, the solvent replaces the vacuum, and the effective forces between macroparticles replace the intermolecular forces. The radial distribution function in Fig. 1 corresponds to a system of charged col-

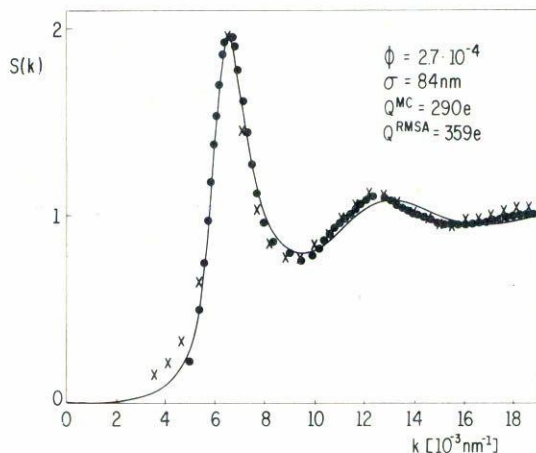


FIGURE 2. Direct comparison between experiment (crosses), computer simulations (dots) and theory (solid line) for the static structure factor  $S(k)$  of a similar sample as in fig. 1.  $Q^{MC}$  and  $Q^{RMSA}$  are the values of the charge  $Q$  employed in the Monte Carlo and in the theoretical calculations, respectively, and were chosen to fit the height of the main peak of the experimental  $S(k)$ , this being the only parameter, not determined accurately otherwise by independent experimental measurements. (Figure reproduced from ref. [18]).

loidal particles of hard-sphere diameter  $\sigma$ , charge  $Q$ , and number concentration  $n$  which interact via an effective pairwise potential modelled by a hard-sphere plus a repulsive screened Coulomb potential. Its specific form is the so-called DLVO (Derjaguin-Landau-Verwey-Overbeek) potential, written as [16,17]

$$u(r) = \frac{Q^2 e^{-\kappa(r-\sigma)}}{\epsilon(1 + \kappa\sigma/2)^2 r}, \quad r > \sigma \quad (1)$$

where  $\epsilon$  is the dielectric constant of the solvent and  $\kappa$  is the Debye screening parameter, which describes the charge-screening due to the counterions and other electrolyte ions in the solution. The dots in Fig. 1 correspond to computer simulations for this model system, and the solid line corresponds to theoretical results [18], based on the use of the “rescaled mean spherical approximation” [19,20]. This is about the simplest, non trivial statistical thermodynamic scheme to calculate  $g(r)$  given the pair potential  $u(r)$ .

A quantity closely related to  $g(r)$  is the static structure factor  $S(k)$ , defined as

$$S(k) = 1 + n \int d^3r [g(r) - 1] e^{i\mathbf{k}\cdot\mathbf{r}}. \quad (2)$$

Just as neutron and x-ray scattering measures directly the static structure factor  $S(k)$  of simple liquids, static light scattering, or x-ray or neutron scattering at

small-angles, may lead to the experimental determination of  $S(k)$  for a colloidal suspension [1,2]. This experimentally-determined  $S(k)$  or  $g(r)$  may be compared directly with theoretical results like those in Fig. 1, and one such comparison is illustrated in Fig. 2. This is the static structure factor of a system similar to that in Fig. 1. This comparison illustrates the degree of accuracy of the current theoretical predictions, as compared with computer and real experimental data [18]. Of course, one should not be left with the impression that all the basic problems referring to the static structure of dispersions have been solved with the same degree of accuracy. In fact, this is currently one of the most active aspects of the study of suspensions, and of complex fluids in general. However, for the purposes of the present discussion, let us assume that the description of the static properties is no longer a problem, so that we can focus our attention in other properties of colloidal suspensions. Furthermore, we shall actually aim at explaining some of those properties in terms, precisely, of the equilibrium static structure represented by  $g(r)$  and  $S(k)$ .

### 3. "Collective" versus "self" diffusion

Brownian motion and diffusion are two intimately related concepts, particularly when referring to highly dilute suspensions. We might say that diffusion is the collective, macroscopic superposition of the Brownian motion of many individual colloidal particles. The most familiar diffusion process is that described by the ordinary diffusion equation,

$$\frac{\partial n(\mathbf{r}, t)}{\partial t} = D_c \nabla^2 n(\mathbf{r}, t), \quad (3)$$

where  $n(\mathbf{r}, t)$  is the instantaneous concentration of colloidal particles at position  $\mathbf{r}$ . This diffusion phenomenon is referred to as "collective" diffusion, since it describes the relaxation of a collective variable. The corresponding diffusion coefficient,  $D_c$ , is known as the "collective" diffusion coefficient.

Quite a different diffusion coefficient characterizes more directly the concept of Brownian motion. The experimental observation of the random motion of *individual* particles must involve the recording of some averaged time-dependent individual property, such as the mean squared displacement,  $\langle(\Delta\mathbf{r}(t))^2\rangle$ , or the velocity auto-correlation function  $\langle\mathbf{V}(t) \cdot \mathbf{V}(0)\rangle$  of individual Brownian particles. It is well known that at sufficiently long times, the mean squared displacement increases linearly with time, and the proportionality constant defines another diffusion coefficient, according to the following expression

$$D_s = \lim_{t \rightarrow \infty} \left[ \frac{\langle(\Delta\mathbf{r}(t))^2\rangle}{6t} \right]. \quad (4)$$

The diffusion coefficient  $D_s$ , thus defined is called the "self-diffusion" coefficient.

The distinction between collective and self-diffusion coefficients would be purely academic if we were to restrict ourselves to infinitely dilute suspensions, as the classical theory of Brownian motion [6–8] does. In the absence of interactions between the Brownian particles, both diffusion coefficients converge to a common value, which we shall denote as  $D^\circ$ , and which is related to the hydrodynamic friction coefficient  $\zeta^\circ$  by Einstein's relation. Thus, in the limit  $n \rightarrow 0$ , we have that

$$D_c = D_s = \frac{k_B T}{\zeta^\circ} \quad (\equiv D^\circ).$$

According to this result, the measurement of  $D_c$  in an ordinary concentration-gradient experiment, in an extremely dilute suspension, leads to an estimate of  $\zeta^\circ$ . The subsequent use of Stokes formula for the friction coefficient of a spherical particle,  $\zeta^\circ = 3\pi\eta\sigma$  (with  $\eta$  being the viscosity of the pure solvent), allows a simple determination of the colloidal particle diameter  $\sigma$ . In fact, particle sizing is one of the most popular practical applications of the classical theory of Brownian motion, although the actual measurement of the diffusion coefficient is carried out nowadays more practically by means of Dynamic Light Scattering (DLS). In these experiments one measures the intermediate scattering function,  $F(k, t)$ , defined as [5]

$$F(k, t) = \frac{1}{V} \langle \delta n(\mathbf{k}, t) \delta n(-\mathbf{k}, 0) \rangle, \quad (6)$$

which is the Fourier transform of the van Hove function of the macrofluid [14], *i.e.*,  $\delta n(\mathbf{k}, t)$  is the spatial Fourier transform of the field of instantaneous concentration fluctuations  $\delta n(\mathbf{r}, t) \equiv n(\mathbf{r}, t) - n$ , and the angular brackets indicate equilibrium ensemble average. If the thermal fluctuations also obey the collective diffusion equation in Eq. (3), it is then a simple exercise (see section 6) to show that  $F(k, t)$  is given by

$$F(k, t) = e^{-k^2 D_c t} S(k), \quad (7)$$

where we have used the fact that  $F(k, 0) = S(k)$  [14]. Actually, with DLS one is not restricted to probe only the relaxation of concentration fluctuations of macroscopic size ( $\sim 1$  mm) and over macroscopic times ( $t \sim 1$  sec). One can also probe [5] the collective diffusion behaviour in the length scale down to the mean interparticle distance between the suspended particles  $n^{-1/3}$  (corresponding to the wave-vector  $k_{\max} = 2\pi n^{1/3}$ , where the main peak of  $S(k)$  is located), and within time scales comparable to the diffusion time  $\tau_I \equiv 10^{-2} n^{-2/3} / D^\circ$  that takes a particle to diffuse a small fraction ( $\sim 10^{-2}$ ) of such mean distance. Clearly, this fact is irrelevant when extremely dilute suspensions are considered, since  $\tau_I \rightarrow \infty$ , as  $n \rightarrow 0$ , and Eq. (7) holds with  $D_s$  given by Eq. (5) for all times. This is, however, no longer the case when the interactions between colloidal particles are not negligible, such as for the systems in Figs. 1 and 2. In this case, the collective diffusion coefficient  $D_c$  actually becomes a spatially and temporally non-local kernel, and the collective diffusion



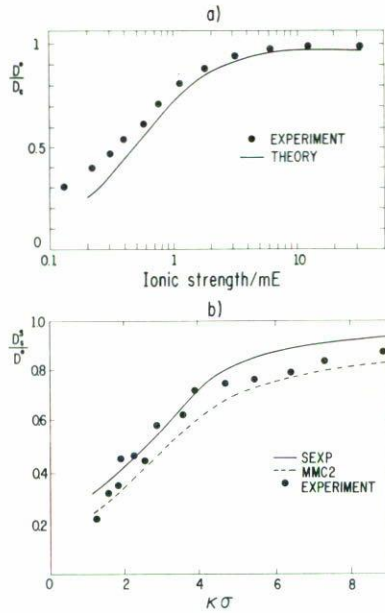


FIGURE 3. (a) Inverse collective diffusion coefficient (in units of  $D^0$ ), as a function of the ionic strength  $I$  of the supporting solution ( $I = \sum_{i=1}^s |Z_i|^2 n_i$ , where  $Z_i$  is the valence of the electrolyte ions of species  $i$ , whose bulk number concentration is  $n_i$ ), for a solution of ganglioside micelles at fixed concentration. The solid line is a theoretical result based on Eq. (7), within the HNC approximation for  $S(0)$  for the DLVO potential. (Reproduced from ref. [21.a]). (b) Self-diffusion coefficient in units of  $D^0$  for a suspension of polystyrene spheres at fixed concentration, as a function of  $I$  (expressed in terms of the inverse Debye screening length  $\kappa \equiv (4\pi e^2 I / \epsilon k_B T)^{1/2}$  and the tracer's diameter  $\sigma$ ) (data taken from ref. [21.b]). The solid and dashed curves are theoretical results explained in section 5.

equation now reads, in general [9],

$$\frac{\partial \delta n(\mathbf{r}, t)}{\partial t} = - \int_0^t dt' \int d^3 r' D(\mathbf{r} - \mathbf{r}'; t - t') \delta n(\mathbf{r}', t'). \tag{8}$$

Thus,  $F(k, t)$  is then given by

$$F(k, t) = \chi(k, t) S(k) \tag{9}$$

where  $\chi(k, t)$  is the spatial Fourier transform of the propagator, or Green's function, of the general collective diffusion equation in Eq. (8). Clearly, Eqs. (3) and (7), with Eq. (5), are the free-diffusion particular case of Eqs. (8) and (9). Another well-known general limiting expression of Eq. (9) is its short-time approximation, which is given

(ignoring hydrodynamic interactions) by [5]

$$F(k, t) = S(k)e^{-k^2 D^\circ t/S(k)} \quad (t/\tau_I \ll 1). \quad (10)$$

This approximation is also exact [9] in the so-called “hydrodynamic” limit, obtained letting  $k \rightarrow 0$  and  $t \rightarrow \infty$ , with  $k^2 t$  remaining constant. In this limit, we recover Eqs. (3) and (7), but with  $D_c$  given not by its free-diffusion limit, Eq. (5), but by the general result [5,9]

$$\begin{aligned} D_c &= D^\circ/S(0) \\ &= D^\circ \left( \frac{\partial \beta P}{\partial n} \right)_\beta, \end{aligned} \quad (11)$$

where the second line makes use of the “compressibility” equation of the theory of liquids [14], which states that  $S(0) = 1/(\partial \beta P/\partial n)_\beta$ , where  $\beta = 1/k_B T$ , and  $P$  is the *osmotic* pressure of the suspension.

In Fig. 3 we reproduce the results of the measurement of  $D_c$  and  $D_s$  in systems similar to those in Figs. 1 and 2. Here, the system is kept at constant concentration, but the Debye screening length  $\kappa^{-1}$  is varied by varying the ionic strength of the supporting solution. Increasing  $\kappa$  increases the screening, and the effects of the interactions become less important. As a result, the system becomes more non-interacting, (*i.e.*,  $(\partial \beta P/\partial n)_\beta \rightarrow 1$ ), and  $D_c$  tends to its free-diffusion value  $D^\circ$  (Fig. 3.a). This Figure also shows the behaviour of the self-diffusion coefficient  $D_s$ , which also approaches  $D^\circ$  as the interactions become less important (Fig. 3.b). Fig. 3 illustrates the fact that  $D_c$  increases and  $D_s$  decreases as a result of the interactions between the Brownian particles. The behaviour of  $D_c$  only reflects the dependence of the thermodynamic factor in Eq. (11), and may then be considered well understood [21.a]. In fact, the solid line in Fig. 3.a is a theoretical calculation based on the HNC approximation [14] for the DLVO pair potential in Eq. (1). The qualitative and quantitative understanding of the behaviour of  $D_s$ , on the other hand, is the subject of intense current research, and is one of the aims of the theory of Brownian motion, as we now discuss.

#### 4. Direct interactions and self-diffusion: facts and intuitive picture

Conventional dynamic light scattering measures the collective intermediate scattering function, Eq. (6). Imagine, however, that under certain circumstances, the vast majority of the particles were not to contribute to the scattering (as would happen, for example, if their refraction index matches that of the supporting solvent), but that the remaining small fraction differ in their optical properties (but in no other respect) from that majority. Then, light would be scattered only by this subset of labelled particles, each of which virtually never encounters another labelled, or “tracer”, particle. This would be a typical self-, or tracer-diffusion experiment, in

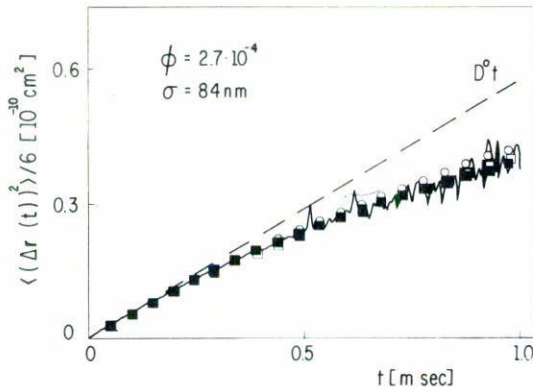


FIGURE 4. Mean-squared displacement  $\langle (\Delta \mathbf{r}(t))^2 \rangle$  of a tracer particle in the suspension in Fig. 2. The noisy curve is the experimental result, the black squares are computer simulations (Brownian dynamics), and the open squares and circles are theoretical results obtained from the two theories described in section 6. The dashed straight line is the free-diffusion result. (Reproduced from ref. [18]).

which the measured property is the *self-diffusion propagator*, defined as [5-9]

$$F_s(k, t) = \left\langle e^{i\mathbf{k} \cdot \Delta \mathbf{r}(t)} \right\rangle, \tag{12}$$

where  $\Delta \mathbf{r}(t)$  is the displacement, during a time interval  $t$ , of a tracer particle. Thus, self-diffusion experiments measure directly the generating function of the probability distribution of the random variable  $\Delta \mathbf{r}(t)$ , and this determines, among other things, the mean squared displacement and the self-diffusion coefficient of that tracer particle interacting with many other identical particles. Fig. 3 is an example of the experimental results which may be obtained with this, or similar, techniques applied to dilute suspensions of highly charged particles. This figure also serves to illustrate that the degeneracy of the free-diffusion limit, in which  $D_c = D_s = D^0$ , is clearly broken by the presence of direct interactions. Explaining why  $D_s < D^0$ , and predicting the extent of this deviation, is one of the goals of the theory of Brownian motion of many coupled Brownian particles. However, as said above, dynamic light scattering also provides the time dependence of quantities such as  $\langle (\Delta \mathbf{r}(t))^2 \rangle$ . Thus, Fig. 4 illustrates a typical signal of an experimental output (solid, noisy curve) for this quantity [18] for the sample whose static structure factor is plotted in Fig. 2. This Figure exhibits the difference between the mean squared displacement in that sample, and the corresponding result for free diffusion, *i.e.*,  $\langle (\Delta \mathbf{r}(t))^2 \rangle = 6D^0 t$  (dashed line). It is immediately clear from this comparison that the main effect of the direct interactions is a departure from the free-diffusion behaviour, which becomes more apparent as time increases, but which is negligible at very short

times. Let us notice, first of all, that the time scale of the Figure ( $t \sim 1$  msec) is far above the typical time  $\tau_B$  associated to the relaxation of the macroparticle velocity,  $\tau_B = \zeta^\circ/M$  (where  $M$  is the mass of the particle), which may be estimated to be around  $10^{-7}$  sec. for the conditions of that sample. Thus, during the times recorded in the experiment,  $t \gg \tau_B$ , and hence, in this time scale, the motion of the particles is purely diffusive. However, in this diffusive regime, only at very short times the mean squared displacement behaves as if it were *free* diffusion. Such short-time regime corresponds to the times in which the tracer diffuses freely in the essentially static field produced by its virtually immobile neighbors, who have had not enough time to change their collective configuration around the tracer. As time ellapses, the dynamic effects of the interactions (*i.e.*, of the “collisions”) with its neighbors cumulate, preventing the tracer from diffusing as fast as if it were diffusing freely. Thus, the interactions of the tracer with its neighbors define another typical time, which we denote by  $\tau_I$ , and which may be defined as the time it takes the tracer to diffuse a small fraction, say one hundredth, of the mean interparticle spacing  $n^{-1/3}$ . Thus, a simple estimate of  $\tau_I$  is given by  $\tau_I = 10^{-2}/(D^\circ n^{2/3})$ , which in our example yields  $\tau_I \approx 2$  msec. For times much longer than  $\tau_I$  (far outside the scale of the Figure), the mean squared displacement once again increases linearly with time, but now with a different, smaller slope. Thus, as a direct consequence of the interactions, we are forced to define *two* self-diffusion coefficients, one associated to the short-time regime,

$$D_s^S \equiv \lim_{t \rightarrow 0} \frac{\langle(\Delta \mathbf{r}(t))^2\rangle}{6t}, \quad (13)$$

(where  $t \rightarrow 0$  means  $t/\tau_I \ll 1$ , but still  $t/\tau_B \gg 1$ ), and another for the asymptotic, long-time behaviour, defined just as in the previous section, (see Eq. (4))

$$D_s^L = \lim_{t \rightarrow \infty} \frac{\langle(\Delta \mathbf{r}(t))^2\rangle}{6t}. \quad (14)$$

Here, of course,  $t \rightarrow \infty$  means  $t/\tau_I \gg 1$ . In the present case, where no hydrodynamic interactions are involved,  $D_s^S$  is identical to the free-diffusion coefficient,  $D^\circ$ , and is independent of the direct interactions, whereas  $D_s^L$  is always smaller than  $D^\circ$ , due precisely to the direct interactions. The experimental results for  $D_s$  in Fig. 3.b correspond, of course, to  $D_s^L$ .

To gain a better intuitive understanding of the difference between  $D_s^S$  and  $D_s^L$ , let us consider the thought experiment illustrated in Fig. 5. Imagine that instead of observing directly the Brownian motion of tracer particles, we could measure the friction force felt by a given particle when we force it to move at a constant velocity  $\mathbf{V}$  through the suspension. Depending on the time- and length-scale of this experiment we would measure a different friction coefficient. For the condition illustrated in Fig. 5.a, in which the particle has not had enough time to collide with other particles, the only frictional forces are those of the solvent, *i.e.*, at short times, the external force  $\mathbf{F}^{\text{ext}}$  needed to move the particle with velocity  $\mathbf{V}$  is given by

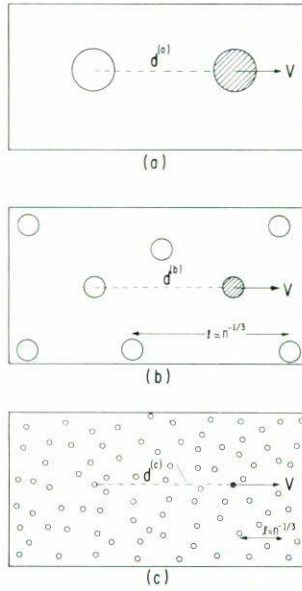


FIGURE 5. Schematic illustration of the motion of a tracer particle moving at constant velocity  $\mathbf{V}$  through a suspension of colloidal particles of number concentration  $n$ , and mean interparticle separation  $\ell = n^{-1/3}$ . The three figures describe the same motion, but in three different time and space scales. In (a), the tracer has suffered a displacement  $d^{(a)}$ , which is much smaller than the mean interparticle spacing  $\ell$ . Thus, in this time-scale, the effect of direct “collisions” with the other particles is still negligible, and the force  $\mathbf{F}^{\text{ext}}$  needed to pull the tracer at constant velocity  $\mathbf{V}$  is given by  $\mathbf{F}^{\text{ext}} = \zeta^S \mathbf{V}$ , where  $\zeta^S$  is the hydrodynamic friction coefficient at short times. In (b), the particle has moved over a distance  $d^{(b)}$  comparable to  $\ell$ , and the effect of collisions start to become appreciable. In (c), the displacement  $d^{(c)}$  is much larger than  $\ell$ , and the force needed to pull the tracer at the same velocity  $\mathbf{V}$  is given by  $\mathbf{F}^{\text{ext}} = (\zeta^S + \Delta\zeta)\mathbf{V}$ , where  $\Delta\zeta\mathbf{V}$  is the additional friction force needed to push the other particles out of the way of the tracer.

$\mathbf{F}^{\text{ext}} = \zeta^S \mathbf{V}$  where  $\zeta^S$  is just the hydrodynamic friction coefficient, given in our case (where we are ignoring hydrodynamic interactions) by its Stokes value,  $\zeta^S = \zeta^0$ . In the opposite regime, Fig. 5.c, the tracer particle has had many encounters with its fellow particles. This produces an additional friction  $\Delta\mathbf{F} = (\Delta\zeta)\mathbf{V}$ , besides the hydrodynamic friction  $\mathbf{F}^S = \zeta^S \mathbf{V}$ . Thus, in this time- and space-regime the external force we would need to apply on the particle to move it at constant velocity  $\mathbf{V}$  is now given by  $\mathbf{F}^{\text{ext}} = (\zeta^S + \Delta\zeta)\mathbf{V}$ , and this defines a long-time friction coefficient,

$$\zeta^L \equiv \zeta^S + \Delta\zeta. \quad (15)$$

The conditions illustrated in Fig. 5.b then describes the transition regime from short-times to long-times, and corresponds to the regime exhibited in Fig. 4. Thus, a complete picture of self-diffusion or self-friction should describe the build-up

of the frictional effects of the direct interactions, and should start with a purely hydrodynamic short-time friction coefficient  $\zeta^S$  (and a corresponding short-time self-diffusion coefficient  $D_s^S = k_B T / \zeta^S$ ), and end up with a long time friction coefficient  $\zeta^L = \zeta^S + \Delta\zeta$  (and a corresponding long-time self-diffusion coefficient  $D_s^L = k_B T / \zeta^L$ ).

The formal theoretical understanding of this dynamic phenomenon was constructed within the last ten years, following essentially a systematic application of corresponding theoretical developments in the dynamics of simple liquids. However, it was only within the last five years that a precise quantitative picture emerged, which led to theoretical results in excellent agreement with the experimental measurements. The state of the art concerning such comparison is illustrated in Fig. 3 and 4, where computer simulation data and theoretical results are also included. The following section contains a description of the theoretical developments which led to those results.

## 5. Theory of self-diffusion

The classical theory of Brownian motion is best described by the ordinary Langevin equation for a freely-diffusing tracer particle [8]

$$M \frac{d\mathbf{V}(t)}{dt} = -\zeta^\circ \mathbf{V}(t) + \mathbf{f}(t), \quad (16)$$

where  $\mathbf{f}(t)$  is a Gaussian, purely random force, representing the thermal fluctuations of the hydrodynamic forces on the particle. The stationarity of the equilibrium state demands that the friction coefficient  $\zeta^\circ$  be related with the correlation function of  $\mathbf{f}(t)$  according to the fluctuation-dissipation relation

$$\langle f_i(t) f_j(0) \rangle = k_B T \zeta^\circ 2\delta(t) \delta_{ij} \quad (i, j = 1, 2, 3). \quad (17)$$

If the tracer particle does not diffuse freely, but is interacting with many other diffusing particles in the suspension, one would expect, following the intuitive picture introduced in the previous section, that besides the hydrodynamic friction and random terms, the direct interactions will lead to an additional friction term and a corresponding fluctuating force, so that Eq. (16) will be modified to read

$$M \frac{d\mathbf{V}(t)}{dt} = -\zeta^S \mathbf{V}(t) + \mathbf{f}^S(t) - \int_0^t dt' \Delta\zeta(t-t') \mathbf{V}(t') + \mathbf{F}(t), \quad (18)$$

where  $\Delta\zeta(t)$  is a memory-function-like friction describing the build-up of the effects of the direct interactions of the tracer with its neighbors, and  $\mathbf{F}(t)$  represents the corresponding random force, generated by the instantaneous departure of the distribution of neighbors from its equilibrium radial distribution  $ng(r)$ . In the following section we provide a derivation of the generalized Langevin Eq. (18), which leads,

upon well-defined approximations, to explicit expressions for  $\Delta\zeta(t)$  in terms of the effective pair potential of the direct interactions and of the equilibrium structural quantities  $g(r)$  and  $S(k)$ .

Once  $\Delta\zeta(t)$  is determined, other relevant properties describing self-diffusion may be calculated. For example, the Laplace transform of the velocity autocorrelation function  $C(t) \equiv \langle \mathbf{V}(t) \cdot \mathbf{V}(0) \rangle / 3$ , denoted as  $C(z)$ , is given by

$$C(z) \equiv \frac{1}{3} \int_0^\infty dt e^{-zt} \langle \mathbf{V}(t) \cdot \mathbf{V}(0) \rangle = \frac{k_B T}{(\zeta^S + \Delta\zeta(z))}, \quad (19)$$

where  $\Delta\zeta(z)$  is the Laplace transform of  $\Delta\zeta(t)$ , and where we have neglected  $z/z_B$  (with  $z_B \equiv M/\zeta^S$ ) in the denominator of the right-hand side. This corresponds, in the time-domain, to the neglect of terms of order  $(\tau_B/t)$  and higher, as it should be done if we wish to describe only the motion of the tracer particle in the diffusive regime. From  $C(t)$  one can easily calculate the mean-squared displacement, since they are related by means of the following equation

$$\langle (\Delta \mathbf{r}(t))^2 \rangle / 6t = \int_0^t dt' (1 - t'/t) C(t'). \quad (20)$$

Clearly, combining Eqs. (20), (19), and the definition of  $D_s^L$  in Eq. (14), we have that the long-time self-diffusion coefficient can be written as

$$D_s^L = \int_0^\infty dt' C(t') = \frac{k_B T}{\zeta^S + \Delta\zeta}, \quad (21)$$

where

$$\Delta\zeta \equiv \Delta\zeta(0) = \int_0^\infty dt \Delta\zeta(t). \quad (22)$$

A still more general program to describe self-diffusion could aim at the calculation of the self-diffusion propagator  $F_s(k, t)$  defined in Eq. (12). The pioneering work of Ackerson [22], Pusey and Tough [6,23], Hess and Klein [9], and others, followed this route, starting from a mesoscopic dynamical description of the coupled Brownian motion of  $N$  colloidal particles, provided by the  $N$ -particle Smoluchowski, Langevin, and Fokker-Planck equations [24,25]. In close analogy with similar developments in simple liquids, they applied well established statistical mechanical formalisms such as projector operators [22], short-time expansions [6], and linear response theory [9]. As a result, they showed that  $F_s(k, t)$  satisfies a memory-function equation, written, neglecting hydrodynamic interactions, as

$$\frac{\partial F_s(k, t)}{\partial t} = -k^2 D^\circ F_s(k, t) + \int_0^t M(k, t - t') F_s(k, t') dt'. \quad (23)$$

Thus, the aim of those theories is to calculate the memory function  $M(k, t)$ . From  $M(k, t)$ , all the previously defined self-diffusion properties follow, since  $M(k, t)$  is such that its Laplace transform  $M(k, z)$  is related  $\Delta\zeta(z)$  by [26]

$$\lim_{k \rightarrow 0} \frac{M(k, z)}{k^2 D^\circ} = \frac{\Delta\zeta(z)}{\zeta^\circ + \Delta\zeta(z)}. \quad (24)$$

Although these statistical mechanical approaches lead to formally exact expressions for  $M(k, t)$  and  $\Delta\zeta(t)$ , their actual application requires the introduction of approximations. The most successful approximate results of this type are the mode-mode coupling approximation introduced by Hess and Klein [9], and the exponential-memory approximation introduced by Arauz-Lara [26–30]. The first is a systematic translation of analogous mode-mode coupling theories of simple liquids, and leads to the following relationship between  $\Delta\zeta(t)$ ,  $F_s(k, t)$ , and the *collective* intermediate scattering function  $F(k, t)$  (Eq. (6))

$$\Delta\zeta(t) = \frac{nk_B T}{3(2\pi)^3} \int d^3k \left[ \frac{kh(k)}{1 + nh(k)} \right]^2 F(k, t) F_s(k, t), \quad (25)$$

in which  $1 + nh(k) = S(k)$  is the static structure factor of the bulk suspension. As we shall explain in the following section, this result can also be derived in an alternative manner, which allows its extension to more general situations. To make Eq. (25) more tractable, the short-time approximation for  $F(k, t)$ , Eq. (10), is introduced, and  $F_s(k, t)$  is approximated either by its short-time limit,

$$F_s(k, t) = e^{k^2 D^\circ t}, \quad (26)$$

or by its long-time expression

$$F_s(k, t) = e^{-k^2 D_s^L t}. \quad (27)$$

The use of Eqs. (25), (10), and (26) leads to an explicit expression for  $\Delta\zeta(t)$  in terms solely of  $S(k)$ . Such an approximation has been labelled MMC1 [26]. The use of Eqs. (27) and (10) in Eq. (25) leads to an expression for  $\Delta\zeta(t)$  in terms of  $S(k)$ ,  $D^\circ$ , and  $D_s^L$ . This expression, when employed in Eqs. (22) and (21), leads to an independent, implicit equation for  $(D_s^L/D^\circ)$ , which must be solved before one can calculate  $\Delta\zeta(t)$ . This second approximate scheme to calculate self-diffusion is labelled MMC2. The only input required in the numerical application of these approximations is then  $S(k)$  and  $D^\circ$ . Since  $S(k)$  has been determined experimentally and theoretically for the system in Fig. 2, the calculation of the mean squared displacement  $\langle(\Delta\mathbf{r}(t))^2\rangle$  is now straightforward. The numerical results, within the MMC2 scheme, are displayed in Fig. 4. Similarly, Fig. 3.b displays the results of the MMC2 approximation for  $D_s^L$  for the conditions of that Figure.



The other approach which has been quite successfully applied to the interpretation of self-diffusion measurements was suggested by Arauz-Lara [27]. It is based on the derivation of exact conditions for the initial value of the memory function  $M(k, t)$  and its first time-derivative. These exact conditions were employed to determine the amplitude and the decay constant of the memory function, modelled by a single exponential function [29]. This leads to approximate expressions for  $M(k, t)$ ,  $\Delta\zeta(t)$ ,  $\langle(\Delta\mathbf{r}(t))^2\rangle$ , and  $D_s^L$ , in terms of  $D^o$ , and of certain integrals involving the pair potential  $u(r)$ , the radial distribution function  $g(r)$ , and the three-particle distribution function  $g^{(3)}(\mathbf{r}_1, \mathbf{r}_2, \mathbf{r}_3)$  [14]. Neglecting terms proportional to  $g^{(3)}(\mathbf{r}_1, \mathbf{r}_2, \mathbf{r}_3)$ , leads to an explicit expressions for those dynamical properties in terms only of  $g(r)$ . Such approximate scheme is referred to as the single-exponential approximation, and it has also been applied to the systems and conditions in Figs. 3.b and 4, where it is labelled SEXP.

As it is clear from the comparison in Figs. 3.b and 4, both methods to describe self-diffusion in terms of the structural properties lead, upon the judicious and well-defined approximations involved, to a successful comparison with experimental and computer simulated results. This is particularly meritorious considering the fact that no fitting parameters are involved in the connections between  $\langle(\Delta\mathbf{r}(t))^2\rangle$  and the static structural properties provided by these theories. Thus, we may conclude that the theory of Brownian motion has been extended to provide a qualitative and quantitative understanding of the effects of direct interactions in suspensions of highly charged particles, where hydrodynamic interactions are negligible.

This optimistic claim is quite fair, as it can be judged by the comparison in Figs. 3.b and 4. Nevertheless, the need arises to extend the range of applicability of these theories to describe additional interaction forces which also affect self-diffusion in systems other than electrostatically correlated systems. In fact, already with charged macroparticles in the limit of infinite dilution, another small frictional effect is apparent, due to the electric interactions with the screening ionic atmosphere, an effect referred to as electrolyte friction. Unfortunately no straightforward extension of the theories discussed in this section, to describe this effect, seems possible. Similarly, the description of the coupled effects of direct and hydrodynamic interactions for concentrated suspensions seems to be a formidable task, if approached along the lines of the theories referred to before. Thus, there is room for alternative theoretical descriptions which allow the extension of the results above to describe these additional friction effects. The following sections review the theoretical methods employed rather recently for such purpose, and its specific applications and results are illustrated in sections 7 and 8.

## 6. Self-diffusion revisited: the generalized Langevin equation

A beautiful generalization of the fundamental ideas of the classical theory of Brownian motion may be found in Onsager and Machlup irreversible thermodynamic theory of fluctuations [31]. Within this scheme, the ordinary Langevin equation, Eq. (16), is just the simplest example of a fluctuation phenomenon cast as a Gauss-

ian Markov stochastic process generated by a linear stochastic differential equation. Within this spirit, we can construct a Langevin-type equation to describe the instantaneous random departures from its equilibrium value, of the local concentration  $n(\mathbf{r}, t)$  of colloidal particles in a suspension. In the previous section, when we said that  $n(\mathbf{r}, t)$  satisfies the diffusion equation, we were actually referring to the average value  $\langle n(\mathbf{r}, t) \rangle$ , whose value at thermodynamic equilibrium is just the bulk number concentration  $n$  for a homogeneous suspension. The instantaneous fluctuations around this average, denoted as

$$\delta n(\mathbf{r}, t) = n(\mathbf{r}, t) - n, \quad (28)$$

satisfies, according to the irreversible thermodynamic theory of fluctuations, a stochastic version of the diffusion equation, which in its simplest form reads [12]

$$\frac{\partial \delta n(\mathbf{r}, t)}{\partial t} = D_c \nabla^2 \delta n(\mathbf{r}, t) - \nabla \cdot \mathbf{j}_{\text{dif}}(\mathbf{r}, t). \quad (29)$$

This equation says that the fluctuations tend to relax to its equilibrium value  $\langle \delta n(\mathbf{r}, t) \rangle = 0$  following the same relaxation law as the average  $\langle n(\mathbf{r}, t) \rangle$ . This is described by the first term on the right-hand side of Eq. (29), which is the analog of the  $-\zeta^\circ \mathbf{V}(t)$  term in the ordinary Langevin equation, Eq. (16). But just as the spontaneous hydrodynamic fluctuations of the supporting solvent give rise to the random force  $\mathbf{f}(t)$  on an isolated Brownian particle, it produces random diffusive fluxes  $\mathbf{j}_{\text{dif}}(\mathbf{r}, t)$  of particles in the suspension, and this is represented by the last term in Eq. (29). These random diffusive fluxes give Eq. (28) the character of a *stochastic diffusion equation*. Furthermore, just as  $\mathbf{f}(t)$  in Eq. (16) is assumed to be a Gaussian,  $\delta$ -correlated noise, we also assume  $-\nabla \cdot \mathbf{j}_{\text{dif}}(\mathbf{r}, t)$  to have those properties, and as a consequence of the stationarity of the equilibrium state, its correlation function is also related with the transport coefficient of the relaxation term (*i.e.*, with  $D_c$ ) by a fluctuation-dissipation relation, which reads [12]

$$\langle (\nabla \cdot \mathbf{j}_{\text{dif}}(\mathbf{r}, t)) (\nabla \cdot \mathbf{j}_{\text{dif}}(\mathbf{r}', t')) \rangle = 2\delta(t - t') D_c n \nabla_r^2 \delta(\mathbf{r} - \mathbf{r}'), \quad (30)$$

where  $\delta(\mathbf{r} - \mathbf{r}')$  is the Dirac delta function.

A simple application of Eq. (29) is the derivation of Eq. (7), which follows after taking the Fourier transform of Eq. (29), multiplying by  $\delta n(-\mathbf{k}, 0)$ , taking the equilibrium average, and using the fact that  $\delta n(\mathbf{r}, 0)$  is statistically independent of the random fluxes  $\mathbf{j}_{\text{dif}}(\mathbf{r}, t)$ . More generally, collective fluctuations are described by Eq. (29), but with the diffusive relaxation term  $D_c \nabla^2 \delta n(\mathbf{r}, t)$  replaced by a spatially and temporally non-local kernel, as in Eq. (8). This leads to the general result in Eq. (9).

Let us now use these ideas to derive the generalized Langevin equation in Eq. (18). As we said before, in self-diffusion experiments, the Brownian motion of a very small fraction of suspended particles is recorded, and each of these tracer particles may be regarded as diffusing independently of the other tracers, while

interacting with the many un-labelled particles in the suspension. Thus, the state of this system may be represented by an equilibrium ensemble of identical systems each containing many identical particles plus a single tracer particle. Let the state of this system be described by the velocity  $\mathbf{V}(t)$  of the tracer, and the local concentration  $n'(\mathbf{r}, t)$  of the other colloidal particles, around the tracer. The vector position  $\mathbf{r}$  in  $n'(\mathbf{r}, t)$  is referred to the center of the tracer, and the prime is a reminder of this fact. In thermodynamic equilibrium, the average value of  $\mathbf{V}(t)$  is  $\langle \mathbf{V}(t) \rangle = \mathbf{O}$ , and the average of  $n'(\mathbf{r}, t)$ , which we shall denote by  $n^{\text{eq}}(r)$ , is just  $ng_{TC}(r)$ , where  $g_{TC}(r)$  is the radial distribution function of the colloidal particles around the tracer. In principle, standard statistical thermodynamic theories [14] may be used to determine  $g_{TC}(r)$ , given the pair potential  $u_{TC}(r)$  of the force between the tracer and any of the other colloidal particles, along with the pair potential  $u_{CC}(r)$  of the colloidal particles. Of course, if the tracer is also identical to the rest of suspended particles, *i.e.*, if  $u_{TC}(r) = u_{CC}(r) = u(r)$ , then  $g_{TC}(r)$  is just the radial distribution function  $g(r)$  of the suspension, an object already discussed and illustrated in section 2.

Let us now write a generalized Langevin equation for the stochastic vector whose components are  $\mathbf{V}(t)$  and  $\delta n'(\mathbf{r}, t)$ . According to the general principles of the irreversible thermodynamic theory [12,31,32], this vector satisfies a linear Langevin-type equation, *i.e.*,  $\mathbf{V}(t)$  and  $\delta n'(\mathbf{r}, t)$  satisfy two coupled stochastic differential equation. The first of them is just a Langevin equation for the tracer [33]

$$M \frac{d\mathbf{V}(t)}{dt} = -\zeta^S \mathbf{V}(t) + \mathbf{f}^S(t) + \int d^3r [\nabla u_{TC}(r)] \delta n'(\mathbf{r}, t). \quad (31)$$

The last term is an *exact* mechanical coupling between  $\mathbf{V}(t)$  and  $\delta n'(\mathbf{r}, t)$ . It is just the total force  $\int d^3r [\nabla u_{TC}(r)] n'(\mathbf{r}, t)$  exerted on the tracer by the other particles instantaneously distributed according to  $n'(\mathbf{r}, t)$ . Since  $n'(\mathbf{r}, t) = n^{\text{eq}}(r) + \delta n'(\mathbf{r}, t)$ , and because of the radial symmetry of  $n^{\text{eq}}(r)$ , only the departures  $\delta n'(\mathbf{r}, t)$  from  $n^{\text{eq}}(r)$  contribute to this force. The other two terms in Eq. (31) represent the force of the solvent on the tracer, which contributes with a dissipative term,  $-\zeta^S \mathbf{V}(t)$ , plus a corresponding Gaussian,  $\delta$ -correlated fluctuating force. With the proper definition of  $\zeta^S$ , which will be given below, Eq. (31) is exact.

The time-evolution equation for  $\delta n'(\mathbf{r}, t)$  constitutes the second linear stochastic equation for the vector  $[\mathbf{V}(t), \delta n'(\mathbf{r}, t)]$ , and has the general form [33]

$$\frac{\partial \delta n(\mathbf{r}, t)}{\partial t} = [\nabla n^{\text{eq}}(r)] \cdot \mathbf{V}(t) - \int_0^t dt' \int d^3r' D'(\mathbf{r}, \mathbf{r}'; t-t') \delta n'(\mathbf{r}', t') - \nabla \cdot \mathbf{j}'_{\text{dif}}(\mathbf{r}, t). \quad (32)$$

The linear term in  $\mathbf{V}(t)$  is an exact (but linearized) streaming term, due to the fact that the vector  $\mathbf{r}$  in  $\delta n'(\mathbf{r}, t)$  is referred to the center of the tracer (which moves with velocity  $\mathbf{V}(t)$ ). The memory term in Eq. (32) is the most general form of the collective diffusion equation (see Eq. (8)), as described from the reference frame of the tracer. The last term represents the corresponding random fluxes. Thus, Eqs. (31) and (32) constitute the most general stochastic linear equation for the vector  $[\mathbf{V}(t), \delta n(\mathbf{r}, t)]$ . (In principle, the dissipative term  $-\zeta^S \mathbf{V}(t)$  should also

involve memory, representing the finite decay time of the hydrodynamic modes of the solvent. Such decay time is, however, much too small in the diffusive regime of interest here, and hence, a constant friction coefficient  $\zeta^S$  suffices).

So far, Eqs. (31) and (32) are exact, although  $\zeta^S$  and  $D'(\mathbf{r}, \mathbf{r}'; t - t')$  have not been yet specified. We could proceed further at this level of generality. Nevertheless, let us replace at this point  $D'(\mathbf{r}, \mathbf{r}'; t - t')$  by its simplest approximation, namely,

$$D'(\mathbf{r}, \mathbf{r}'; t - t') = -2\delta(t - t')D_c\nabla^2\delta(\mathbf{r} - \mathbf{r}'), \tag{33}$$

which allows us to write Eq. (32) as

$$\frac{\partial\delta n'(\mathbf{r}, t)}{\partial t} = [\nabla n^{\text{eq}}(r)] \cdot \mathbf{V}(t) + D_c\nabla^2\delta n'(\mathbf{r}, t) - \nabla \cdot \mathbf{j}'_{\text{dif}}(\mathbf{r}, t). \tag{34}$$

This means that we have assumed that the diffusive relaxation of  $\delta n'(\mathbf{r}, t)$  is described by the same law as the bulk collective fluctuations in Eq. (29), and that the random fluxes are modelled as the Gaussian,  $\delta$ -correlated fluctuating fluxes explained in the context of that equation, which is recovered if we set  $\mathbf{V}(t) = 0$  in Eq. (34). This assumption is a reasonable simplification, although it involves a rather crude description of the dynamics of  $\delta n'(\mathbf{r}, t)$ . However, we introduce it here only to illustrate the procedure that follows.

Let us now apply the idea of contraction of the description [12,32,34], which in this example amounts to solving Eq. (34) for  $\delta n(\mathbf{r}, t)$  in terms of  $\mathbf{V}(t)$ , and substituting the result in the last term of Eq. (31). This eliminates  $\delta n'(\mathbf{r}, t)$ , leading to a closed equation for  $\mathbf{V}(t)$  that has the structure announced in Eq. (18). Mathematically, Eq. (34) is just an inhomogeneous ordinary diffusion equation, whose solution can be written as

$$\begin{aligned} \delta n(\mathbf{r}, t) = & \int_0^t dt' \int d^3r' \chi'(\mathbf{r}, \mathbf{r}'; t - t') [\nabla' n^{\text{eq}}(r')] \cdot \mathbf{V}(t) \\ & + \int_0^t dt' \int d^3r' \chi'(\mathbf{r}, \mathbf{r}'; t - t') [-\nabla \cdot \mathbf{j}'_{\text{dif}}(\mathbf{r}', t)] \\ & + \int d^3r' \chi(\mathbf{r}, \mathbf{r}'; t) \delta n(\mathbf{r}, 0), \end{aligned} \tag{35}$$

where  $\chi'(\mathbf{r}, \mathbf{r}'; t - t')$  is the collective diffusion propagator,

$$\chi'(\mathbf{r}, \mathbf{r}'; t) = (4\pi D_c t)^{-3/2} \exp[-(\mathbf{r} - \mathbf{r}')^2/4D_c t], \tag{36}$$

*i.e.*, it is the solution of the homogeneous diffusion equation whose initial condition

is  $\chi'(\mathbf{r}, \mathbf{r}'; 0) = \delta(\mathbf{r}, \mathbf{r}')$ . Substituting Eq. (35) in Eq. (31), we obtain

$$M \frac{d\mathbf{V}(t)}{dt} = -\zeta^S \mathbf{V}(t) + \mathbf{f}^S(t) - \int_0^t dt' \Delta\zeta(t-t') \mathbf{V}(t') + \mathbf{F}(t), \quad (37)$$

where the memory-function term derives from the first term on the r.h.s. of Eq. (35), and where we have defined the time-dependent friction  $\Delta\zeta(t)$  as

$$\Delta\zeta(t) = -\frac{1}{3} \int d^3r \int d^3r' [\nabla u_{TC}(t)] \cdot \chi'(\mathbf{r}, \mathbf{r}'; t) [\nabla' n^{\text{eq}}(r')]. \quad (38)$$

The other terms, which derive from the second and third terms of the r.h.s. of Eq. (35), are linear on the random variables  $-\nabla \cdot \mathbf{j}_{\text{dir}}(\mathbf{r}, t)$  and  $\delta n'(\mathbf{r}, 0)$ , respectively, and have been grouped in the last term,  $\mathbf{F}(t)$ , of Eq. (37). This is, hence, a random force, which originates from the spontaneous departures of the distribution of colloidal particles around the tracer from its radial equilibrium average  $n^{\text{eq}}(r)$ . Equations (37) and (38) constitute the most fundamental results of the theory presented here, and in the following we elaborate further on some aspects of its derivation and generality.

The derivation above is a simple exercise of the idea of “contraction of the description”, in which the aim is to establish a connection between two phenomenological levels of description of the same fluctuation phenomenon, which differ only in their degree of detail [32,34]. Thus, we started with a system of two coupled equations of motion for the state variables  $\mathbf{V}(t)$  and  $\delta n'(\mathbf{r}, t)$ , cast as a Markov stochastic process. This constitutes the non-contracted description. In eliminating  $\delta n'(\mathbf{r}, t)$ , we have carried out the contraction procedure. This resulted in a Langevin equation for  $\mathbf{V}(t)$  alone, which exhibits memory as a consequence of the contraction. In principle, however, the non-contracted description itself should be non-local in time as indicated in Eq. (20), since it could be viewed as the result of a primary contraction from a Hamiltonian level of description [35]. Such considerations are important, since the dynamics of the fluctuations in the local concentration of colloidal particles is known to involve memory effects [5,9] of the type in Eqs. (32) and (8), and which are not included in the simple diffusion model employed in Eq. (34).

Prompted by these considerations, in a recent work [33] we have indicated a canonical procedure to carry out the contraction from a non-Markovian level of description. This procedure is based on the use of general conditions imposed by the stationarity condition on the structure of the generalized Langevin equations that defines such a stationary non-Markovian process (*i.e.*, Eqs. (31) and (32) in our problem). These conditions, along with others that derive from the time-reversal symmetry properties of the dynamic variables themselves, lead to precise “selection rules” for the “frequency”, “memory”, and “random force” terms, which are extensions of the well-known Onsager-Casimir relations [12,13]. We have applied those selection rules to our problem, within the assumption that the only dissipative processes to be considered are the diffusion of the cloud of colloidal particles and the hydrodynamic friction on the tracer. As a result of such analysis [33], one concludes,

in particular, that the simultaneous presence of the cross-coupling, non-dissipative terms in Eqs. (31) and (32) is required by one of the general selection rules referred to above, which also requires [33] the following relation to be fulfilled

$$\nabla n^{\text{eq}}(r) = -\frac{1}{k_B T} \int d^3 r' \sigma(\mathbf{r}, \mathbf{r}') \nabla' u_{TC}(r'), \quad (39)$$

where  $\sigma(\mathbf{r}, \mathbf{r}')$  is the equal-time correlation function of  $\delta n'(\mathbf{r}, t)$ , *i.e.*,

$$\sigma(\mathbf{r}, \mathbf{r}') = \langle \delta n(\mathbf{r}, 0) \delta n(\mathbf{r}', 0) \rangle. \quad (40)$$

Eq. (39) is, however, an exact relationship, well-known in the statistical-mechanical literature of inhomogeneous fluids [14,36].

Once we are sure that the time-evolution equations which constitute our non-contracted description do not violate any of the mentioned selection rules, the contraction procedure is rather straightforward [33], and follows a similar route as that in our simple derivation, thus leading essentially to the same results, namely, Eqs. (37) and (38). In fact, the only difference is that the propagator  $\chi'(\mathbf{r}, \mathbf{r}'; t)$  in Eq. (38) is no longer given just by Eq. (36). Instead, it is the solution of the more general diffusion equation,

$$\frac{\partial \chi'(\mathbf{r}, \mathbf{r}''; t)}{\partial t} = - \int_0^t dt' \int d^3 r' D'(\mathbf{r}, \mathbf{r}'; t-t') \chi'(\mathbf{r}', \mathbf{r}''; t') \quad (41)$$

with the initial condition  $\chi'(\mathbf{r}, \mathbf{r}'; 0) = \delta(\mathbf{r} - \mathbf{r}')$ .

An important requirement of the stationarity condition on the structure of a generalized Langevin equation is the existence of a fluctuation-dissipation relation between the generalized relaxation kernel and the random term [32]. For the particular case of the generalized Langevin equation represented by the system of coupled Equations (31) and (32), such fluctuation-dissipation relation reads

$$\langle f_i^S(t) f_j^S(0) \rangle = M k_B T \zeta^S \delta(t) \delta_{ij} \quad (42)$$

$$\langle [\nabla \cdot \mathbf{j}'_{\text{dif}}(\mathbf{r}, t)] [\nabla' \cdot \mathbf{j}'_{\text{dif}}(\mathbf{r}', 0)] \rangle = \int d^3 r'' D'(\mathbf{r}, \mathbf{r}''; t) \sigma(\mathbf{r}'', \mathbf{r}') \quad (43)$$

for  $i, j = 1, 2, 3$  and  $\mathbf{r}, \mathbf{r}' \in R^3$ . These relations can be employed to demonstrate the fluctuation-dissipation theorem that holds at the contracted level, which reads [33]

$$\langle F_i(t) F_j(0) \rangle = M k_B T \Delta \zeta(t) \delta_{ij} \quad (i, j = 1, 2, 3). \quad (44)$$

Let us also notice that by using Eq. (39) into Eq. (38) one can derive two alternative (but formally equivalent) expressions for  $\Delta \zeta(t)$  in terms of  $\sigma(\mathbf{r}, \mathbf{r}')$  and  $\chi'(\mathbf{r}, \mathbf{r}'; t)$  [33]. The first involves only  $[\nabla u_{TC}(r)]$ , and the second, which will be used

below, reads

$$\Delta\zeta(t) = \frac{k_B T}{3} \int d^3 r \int d^3 r' [\nabla n^{\text{eq}}(r)] \cdot [\sigma^{-1} \chi'(t)](\mathbf{r}, \mathbf{r}') [\nabla n^{\text{eq}}(r')], \quad (45)$$

where the function  $[\sigma^{-1} \chi'(t)](\mathbf{r}, \mathbf{r}')$  is the convolution of  $\sigma^{-1}$  and  $\chi'(\mathbf{r}, \mathbf{r}'; t)$ , with  $\sigma^{-1}(\mathbf{r}, \mathbf{r}')$  being the inverse function of  $\sigma(\mathbf{r}, \mathbf{r}')$  (i.e., their convolution equals the Dirac delta function). Both quantities,  $\sigma(\mathbf{r}, \mathbf{r}')$  and  $\chi'(\mathbf{r}, \mathbf{r}'; t)$ , depend on  $\mathbf{r}$  and  $\mathbf{r}'$  separately, since the field  $u_{TC}(r)$  breaks the homogeneity of space near the tracer particle.

Finally, let us notice that for short times, i.e., times short enough for  $\chi'(\mathbf{r}, \mathbf{r}'; t)$  not to depart appreciably from  $\delta(\mathbf{r} - \mathbf{r}')$ , the time-dependent friction-function equals approximately  $\Delta\zeta(0)$ ,

$$\Delta\zeta(0) = \frac{1}{3} \int d^3 r [\nabla^2 u_{TC}(r)] n^{\text{eq}}(r) \equiv k_H, \quad (46)$$

which is the spring constant of the approximately harmonic force on the tracer originating from its interaction with its virtually static neighbours, distributed according to  $n^{\text{eq}}(r)$ . The Brownian motion that the tracer executes in such harmonic cage during this short-time regime is described by the following Langevin equation

$$M d\mathbf{V}(t)/dt = -\zeta^S \mathbf{V}(t) + \mathbf{f}^S(t) - k_H (\Delta \mathbf{r}_T(t)), \quad (47)$$

where  $\Delta \mathbf{r}_T(t) = \int_0^t \mathbf{V}(t') dt'$  is the tracer's displacement. Equation (47) follows from averaging Eq. (37) over initial concentration fluctuation profiles  $\delta n'(\mathbf{r}, 0)$ , and recognizing the fact that even for these short times, the time integral of the random flux term  $-\nabla \cdot \mathbf{j}'_{\text{dif}}(\mathbf{r}, t)$  vanishes. Thus, if we denote by  $D_s^S$  the diffusion coefficient which describes the Brownian motion of the tracer in this short time regime, then from Equation (47) we have that  $D_s^S$  is given by  $D_s^S = k_B T / \zeta^S$ . Here we have employed the same symbol for  $k_B T / \zeta^S$  as for the short-time self-diffusion coefficient defined in Eq. (13). This is not, of course, a loose notation, but the recognition of an important fact: the short-time self-diffusion coefficient  $D_s^S$  describes, according to its definition in Eq. (13), the Brownian motion of the tracer in the same time-regime where Eq. (47) is valid. Thus,  $D_s^S$  and  $k_B T / \zeta^S$  are one and the same thing. As a consequence, we have now given a well-defined meaning to the phenomenological coefficient  $\zeta^S$ , heretofore left undetermined. This identification of  $\zeta^S$  with  $k_B T / D_s^S$  also provides the means for its experimental determination as the initial slope of  $\langle (\Delta \mathbf{r}(t))^2 \rangle / 6t$  in the diffusive regime. Of course, as indicated in Fig. 4,  $D_s^S = D^\circ$  for highly dilute suspensions of strongly charged particles, where hydrodynamic interactions are negligible. Thus, in this case,  $\zeta^S = \zeta^\circ$ , where  $\zeta^\circ$  is the Stokes friction coefficient of the tracer. However, when hydrodynamically concentrated dispersions are considered, the identification above becomes most relevant, as we discuss in the following section.

To proceed further we must introduce approximations such as those involved in our simple model in Eq. (34). The most essential ones concern the expression employed for the collective diffusion propagator  $\chi'(\mathbf{r}, \mathbf{r}'; t)$ . Before we commit ourselves to any particular approximation for this quantity let us notice that a general simplification results if we assume that  $\chi'(\mathbf{r}, \mathbf{r}'; t)$  and  $\sigma(\mathbf{r}, \mathbf{r}')$  depend on  $\mathbf{r}$  and  $\mathbf{r}'$  only through the distance  $|\mathbf{r} - \mathbf{r}'|$ . This amounts to ignoring the effects of the field of the tracer in the calculation of these quantities. This approximation, which we shall refer to as the “homogeneous fluid approximation” [33], is involved in the specific results presented in this paper. Under those circumstances, Eq. (45) can also be written as

$$\Delta\zeta(t) = \frac{k_B T n}{24\pi^3} \int d^3k [(kh_{TC}(k))^2 / S(k)] \chi'(k, t), \quad (48)$$

where  $h_{TC}(k)$  is the Fourier transform of  $[n^{eq}(r)/n - 1]$ , and  $S(k) = 1 + nh_{CC}(k) = \sigma(k)/n$  is the static structure factor of the diffusing particles, *i.e.*,  $\sigma(k)$  is the Fourier transform of the isotropic function  $\sigma(|\mathbf{r} - \mathbf{r}'|)$ . Similarly,  $\chi'(k, t)$  is the Fourier transform of the collective diffusion propagator.

The next approximation involves the prime on  $\chi'(k, t)$ . We have consistently denoted properties described from the reference frame of the tracer by a prime. The exact relationship between the primed quantities and the corresponding (unprimed) properties described from a fixed reference frame is unknown. Thus, here we also require approximations. For example, one can compare the definition of  $\chi(k, t)$  and of  $\chi'(k, t)$ , and neglect in this comparison the correlation between the displacement of the tracer,  $\Delta\mathbf{r}_T(t)$ , and the local concentration fluctuations  $\delta n(\mathbf{r}, t)$ . As a result one is led [33] to the following approximation

$$\chi'(k, t) = F_T(k, t)\chi(k, t), \quad (49)$$

where the “tracer-diffusion propagator”  $F_T(k, t)$  is defined as

$$F_T(k, t) = \exp[i\mathbf{k} \cdot \Delta\mathbf{r}_T(t)], \quad (50)$$

*i.e.*, it is the self-diffusion propagator of Eq. (12) in the particular case that the tracer is identical to the other particles. The expression for  $\Delta\zeta(t)$  which results from employing Eq. (49) into Eq. (48) will be referred to as the mode-mode coupling approximation, in reference to the fact that it was first suggested by Hess and Klein [9] using mode-mode coupling arguments, for the particular case of self-diffusion. Clearly, taking Eq. (49) into Eq. (48), and recalling Eq. (9), we can see that Eq. (48) reduces to Eq. (25) in that particular case, namely, when  $h_{TC}(k) = h_{CC}(k) = h(k) = (S(k) - 1)/n$ . As argued after Eq. (25), we still have to approximate  $\chi(k, t)$  and  $F_T(k, t)$ . The pertinent approximations leading to the MMC1 and MMC2 schemes were defined there, and their quantitative results were already discussed in connection to Fig. 3.



Of course, the purpose of the present section is not only to provide a simple derivation of an otherwise well established result, but to pave the way to extend the theory of Brownian motion to still more interesting situations. Already Eq. (48) contains a relevant generalization, to the case when the tracer is not identical to the other colloidal particles in the suspension. But more important, the extension to the case in which the suspension contains particles of various species turns out to be rather straightforward within the approach described here. Such an extension is employed in section 8 to describe electrolyte friction. First, however, we discuss the application of these results to systems with strong hydrodynamic interactions.

## 7. Concentrated hard-sphere suspensions

Let us now consider a different kind of suspension than the dilute but electrostatically correlated systems dealt with above. Dispersions of neutral macroparticles in organic solvents, with adequate refractive-index matching, may be manufactured [37,38], which behave like model hard-sphere suspensions. In these systems, the direct interactions are the hard-sphere repulsion determined by the physical diameter of the particles. The typical concentrations in these systems may be quite high, so that the volume fraction  $\phi$  may be as large as 0.5, above which the direct interactions drive crystallization or glass formation [37]. At such high volume fractions, however, hydrodynamic interactions become a most important feature of the dynamical properties of these systems, and in this sense they represent an opposite extreme case from the electrostatically correlated suspensions considered above. The fact that hydrodynamic interactions cannot be described by pairwise additive effective interactions [10,11,39] renders the description of their effects a genuine and complex many-body problem. Nevertheless, this problem has been approached by several authors [10,11,39–42], and as a result, a good theoretical understanding has emerged of the effect of these non-dissipative forces on their short-time self-diffusion properties [39,40].

On the other hand, dynamic light scattering techniques have been recently applied [37,38] to the determination of the time-dependence of the mean-squared displacement of labelled particles in these suspensions. Fig. 6 illustrates the main features of such measurements. In this figure,  $\langle(\Delta\mathbf{r}(t))^2\rangle$  is plotted for different values of the volume fraction. As a reference, the free-diffusion result ( $\phi = 0$ ) is also indicated. The first thing we notice, is that each curve seems qualitatively rather similar to the result in Fig. 4, where there were strong electrostatic direct forces, but no hydrodynamic interactions. There is, however, a fundamental difference: In Fig. 6, none of the curves approaches the free-diffusion behaviour at short times, as the system in Fig. 4 does. As a consequence, if we determine the short-time self-diffusion coefficient according to its definition in Eq. (13), *i.e.*, from the initial slope of  $\langle(\Delta\mathbf{r}(t))^2\rangle$ , we get from Fig. 4 that  $D_s^S = D^0$ , independently of the direct interactions, whereas from Fig. 6 we find that  $D_s^S$  is a function of volume fraction. This is the first relevant observation deriving from the experimental data in Fig. 6. A summary of the corresponding short-time results for different volume fractions

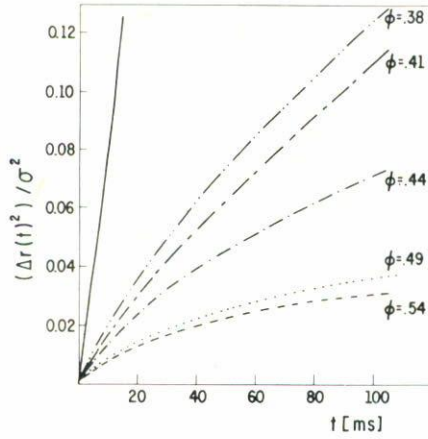


FIGURE 6. Experimentally measured mean-squared displacement in a suspension of hard-sphere particles of diameter  $\sigma$  at various volume fractions as a function of time. The solid straight line corresponds to free diffusion. (Reproduced from ref. [37]).

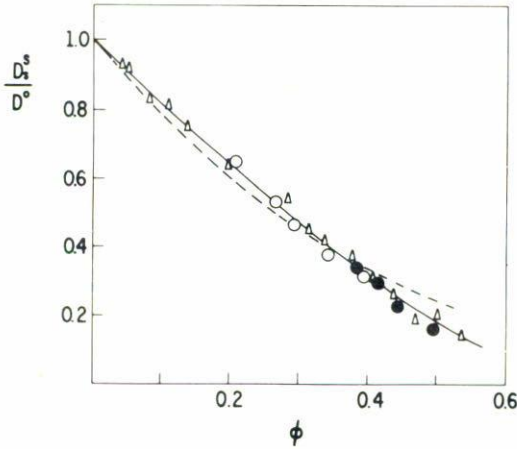


FIGURE 7. Short-time self-diffusion coefficient  $D_s^S$  in units of  $D^0$ , as a function of volume fraction, for various hard-sphere suspensions differing in their hard-sphere size (various symbols). The solid line is an empirical fit, and the dashed line is the theoretical result of ref. [41]. (Reproduced from ref. [37]).

is plotted in Fig. 7, where the  $\phi$ -dependence of  $D_s^S$  for hard-sphere suspensions is illustrated. In that figure, the various symbols corresponds to samples [37] which differ in the size of the colloidal particles. Thus, we learn another important fact: For hard-sphere suspensions,  $D_s^S / D^0$  does depend only on  $\phi$ , and not separately on  $n$  and  $\sigma$ , which is a nice scaling property expected in genuine hard-sphere systems.

As we said before, important advances have been made in the theoretical understanding of the short-time effects of hydrodynamic interactions, and the result of the theory of Beenaker and Mazur [39,41] are also plotted in Fig. 7. In a simple way to understand these effects, one can say that the presence of the Brownian particles modify the effective viscosity felt by any of the particles, so that the friction coefficient describing the short-time diffusion is still given by the Stokes expression, but with an effective, volume-fraction dependent viscosity [42], which is affected rather weakly by the direct interactions [31]. In summary, from the results in Fig. 7 we learn that concerning short-time self-diffusion the volume-fraction dependence of  $D_s^S$  in these systems is amenable to experimental determination, and its theoretical understanding may be qualified as acceptable, probably awaiting only further quantitative refinements.

Understanding the intermediate and long-time behaviour of  $\langle(\Delta\mathbf{r}(t))^2\rangle$  observed in the experimental data in Fig. 6 represents, on the other hand, a still more challenging theoretical problem than the purely hydrodynamic effects involved in  $D_s^S(\phi)$ . According to the conventional approaches employed to describe self-diffusion [5,9,26–30], except at short-times, the effects of hydrodynamic and direct interactions intermingle in such a complex manner that no simple scheme seems at sight to decouple them. Thus, any effort made to understand self-diffusion at longer times is particularly valuable at this stage. It is in this sense that the theoretical approach explained in the previous section constitutes much more than a re-derivation and extension of otherwise available results for systems without hydrodynamic interactions.

The theory described in section 6 is based, precisely, on the existence of well separated time-scales, such that at short times a single quantity, namely,  $\zeta^S$ , is the relevant parameter. The theory has the limitation of not providing the means to calculate a priori this parameter. It has the virtue, however, that it provides a precise definition for it, which is just  $k_B T/D_s^S$ . This property, as we just saw, happens to be readily measurable experimentally. Furthermore, the very writing of Eq. (31) involves already a neat decoupling between the short-time hydrodynamic effects (represented by  $\zeta^S$ ) and the effects of direct interactions, entering in the last term of that equation. This decoupling is a fundamental aspect of the generality of the main results in Eqs. (37) and (38). This allows us to apply those results to our present case in a rather simple manner, *i.e.*, taking  $\zeta^S$  as an experimentally determined quantity, given, for example, by the results in Fig. 7, with  $\zeta^S = k_B T/D_s^S$ .

Of course, a similar decoupling should be made in the second equation on which the theory is based, namely, Eq. (32). In this case, no similarly general and exact arguments have been given, but a reasonable and consistent approximation [43,44] can be provided, namely, that also for collective diffusion one should replace  $D^\circ$  by  $D_s^S$  when hydrodynamic interactions are considered. This allows us to use particular approximate schemes, such as the mode-mode coupling approximation explained in Eq. (48), or more particularly in Eqs. (25–27). From these results we could calculate  $\Delta\zeta(t)$ ,  $\langle(\Delta\mathbf{r}(t))^2\rangle$ ,  $D_s^L$ , etc., in terms only of  $D_s^S$  and  $S(k)$ . Such results could then be compared with experimental measurements like those in Fig. 6.

In Fig. 8 we illustrate one such comparison. The data in this figure are the values for  $D_s^L$  scaled with the free-diffusion coefficient  $D^\circ$  as a function of  $\phi$ . According

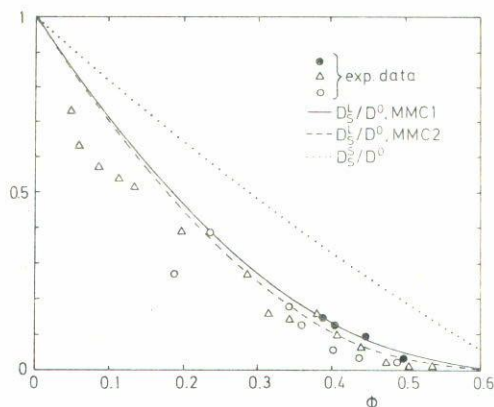


FIGURE 8. Long-time self-diffusion coefficient  $D_s^L$  in units of  $D^0$  for hard-sphere suspensions. The solid and the dashed lines are the theoretical results obtained from the MMC1 and MMC2 approximate theoretical schemes. The various symbols represent the experimental results from various samples differing in their hard-sphere diameters. For comparison, the empirical fit in Fig. 7 for  $D_s^S/D^0$  is also plotted (dotted line). (Experimental data taken from ref. [37]).

to its definition,  $D_s^L$  should be read from the asymptotic, final slope of  $\langle(\Delta\mathbf{r}(t))^2\rangle$  plotted as a function of time, as in Fig. 6. The theoretical results presented in Figure 8 were calculated using the MMC1 and the MMC2 approximations, with  $S(k)$  calculated from the Percus-Yevick approximation [14], and with  $D_s^S$  taken from the experimental data in Fig. 7. Clearly, the agreement between theory and experiment cannot be better, given the fact that absolutely no adjustable parameters are involved in the theoretical calculation.

Although more extensive comparisons of this sort are clearly desirable, the main limiting step in this direction is at the moment the production of more abundant and precise experimental results. Because of its simplicity, the predictions of the theory in other cases, such as when the tracer is not identical to the other particles, or when polydisperse suspensions are considered, can be calculated with relatively little effort. Still, let us emphasize the fact that the theoretical results presented in Fig. 8 stand, at the moment, like the only predictions for long-time self-diffusion properties at volume fractions far from the linear regime in  $\phi$  [40]. This is already a relevant step in our way to understand one of the most fundamental problems posed by this type of complex fluid, in terms of relatively simple and physically intuitive terms.

## 8. Electrolyte friction

A third example of the application of the general results derived in section 6 is the description of electrolyte friction. Here we return to suspensions of highly charged

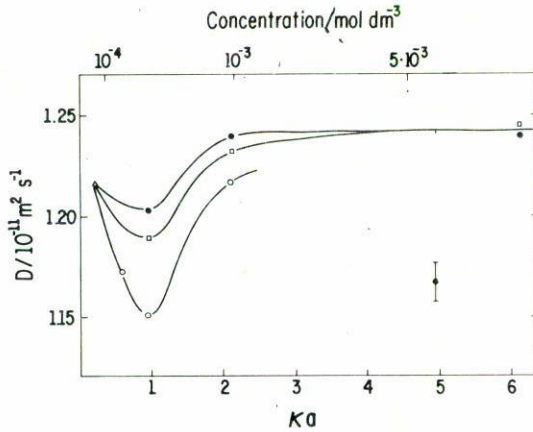


FIGURE 9. Diffusion coefficient of isolated polystyrene spheres diffusing in an ionic solution of varying electrolyte concentration, as a function of  $\kappa a$  (where  $a$  is the radius of the spheres). The three curves correspond to three different types of added electrolyte. (Reproduced from ref. [45]).

particles in an aqueous electrolyte solution, but under conditions of extreme dilution of colloidal particles. In this case, the direct and hydrodynamic interactions between the suspended macroions are negligible, and thus,  $D_s^L = D_s^S = k_B T / \zeta^S$  where  $\zeta^S$  should be identical, if the particles were not charged, to the Stokes friction coefficient  $\zeta^o$ . Due to the electrostatic interactions between the macroion and its counterions (and the small ions of the supporting ionic solution),  $\zeta^S \neq \zeta^o$ . In Fig. 9 we reproduce the results of measurement of  $D$  ( $\equiv D_s^L = D_s^S$ ) for freely diffusing polystyrene spheres in an ionic solution of varying ionic strength [45]. The first thing that we notice is that  $D$  is not a constant, but it depends on the amount of electrolyte ions. Second, we notice that there is a well-defined minimum of  $D$  at  $\kappa a \approx 1$ , where  $a$  is the macroparticle radius and  $\kappa$  is the inverse Debye screening length ( $\kappa^2 = (4\pi\epsilon/k_B T) \sum_i n_i q_i^2$ , where  $n_i$  and  $q_i$  are the number concentration and charge of the small ions of species  $i$ ). These results may be understood as the manifestation of the additional friction,  $-\Delta\zeta^{\text{el}}V(t)$ , besides the pure solvent friction  $-\zeta^o V(t)$  (where  $\zeta^o = 6\pi\eta a$ ), due to the interactions between the macroion and its own ionic cloud. Thus, the measured self-diffusion coefficient may be written as

$$D = \frac{k_B T}{\zeta^o + \Delta\zeta^{\text{el}}}, \quad (51)$$

where  $\Delta\zeta^{\text{el}}$  is called the “electrolyte friction”. Electrolyte friction is generally a much smaller effect than the self-friction induced by polyion-polyion interactions in less dilute suspensions, like those considered earlier in this paper. Thus, our earlier assumption in that case, that the short-time self-diffusion coefficient  $D_s^S$  could be

approximated by  $D^0$ , and not by Eq. (51), turned out to be a good approximation. Fig. 9 shows, however, that electrolyte friction effects can also be observed experimentally under appropriate conditions.

The theoretical calculation of  $\Delta\zeta^{\text{el}}$  has a rather long history. Already in 1954, Booth [46] provided the first description of this effect, by calculating  $\Delta\zeta^{\text{el}}$  as the net electrostatic force on a macroion moving at constant velocity due to its interactions with its distorted ionic atmosphere. This still constitutes the main theoretical approach to the description of electrolyte friction [47], although its extension to non-stationary motion of the polyion remains a challenging problem. Furthermore, the connection between this relaxation effect and the effects of spontaneous fluctuations, measured in the light-scattering experiments illustrated in Fig. 9, has not been fully clarified. On the other hand, Schurr [48] provided the first theoretical description of electrolyte friction effects on the Brownian motion of isolated polyions. Although his approach made use of rather severe approximations at a very early stage, his final result for  $\Delta\zeta^{\text{el}}$  yields a remarkably simple analytic expression for  $\Delta\zeta^{\text{el}}$  as a function of  $\kappa a$ . Both of the theories just mentioned predict the main feature observed in Fig. 9, namely, a maximum of  $\Delta\zeta^{\text{el}}$  (and a corresponding minimum of  $D$ ) at  $\kappa a \approx 1$ .

The general results of section 6 may also be extended to describe electrolyte friction, and this application leads not only to expressions for  $\Delta\zeta^{\text{el}}$ , but also to expressions for the dynamical version of this quantity. The main results of section 6 must first be extended to the general case when the tracer diffuses in a suspension containing more than one species of Brownian particles. This is, however, a rather straightforward extension. It leads, for example (see Eq. (38)), to

$$\Delta\zeta(t) = -\frac{1}{3} \sum_{i=1}^s \sum_{j=1}^s \int d^3r \int d^3r' [\nabla u_{Ti}(r)] \cdot \chi_{ij}(\mathbf{r}, \mathbf{r}'; t) [\nabla' n_j^{\text{eq}}(r')], \quad (52)$$

when there are  $s$  species of colloidal particles, interacting through a central pair potential  $u_{Ti}(r)$  with the tracer, and whose radial distribution function around the tracer is  $g_{Ti}(r) = n_i^{\text{eq}}(r)/n_i$  (where  $n_i$  is the bulk concentration of species  $i=1,2,\dots,s$ ). In Eq. (52),  $\chi_{ij}(\mathbf{r}, \mathbf{r}'; t)$  is the collective-diffusion propagator, *i.e.*, it is defined by the following equation

$$\langle \delta n_i(\mathbf{r}, t) \delta n_j(\mathbf{r}', 0) \rangle = \sum_{k=1}^s \int d^3r'' \chi_{ik}(\mathbf{r}, \mathbf{r}''; t) \sigma_{kj}(\mathbf{r}'', \mathbf{r}'), \quad (53)$$

and is such that  $\chi_{ij}(\mathbf{r}, \mathbf{r}'; t=0) = \delta_{ij} \delta(\mathbf{r}-\mathbf{r}')$ . Clearly,  $\sigma_{ij}(\mathbf{r}, \mathbf{r}')$  is just the equal-time correlation function  $\langle \delta n_i(\mathbf{r}, 0) \delta n_j(\mathbf{r}', 0) \rangle$  of the fluctuations in the local concentration of species  $i$  and  $j$ .

The application of these results to describe electrolyte friction [49–51] is based on the fact that the small ions, without being large Brownian particles, they do, anyway, undergo Brownian motion and diffusion. Hence, the result in Eq. (52) also holds to describe the friction effects produced on the polyion by the counterions and the various other species of electrolyte ions, with which it interacts through the

unscreened Coulomb potential

$$u_{Ti}(r) = \begin{cases} \frac{Qq_i}{\epsilon r}, & r > a + a_i \\ \infty, & r < a + a_i \end{cases} \quad (54)$$

with  $\epsilon$  being the dielectric constant of the solvent, and where  $a_i$  is the radius of the small ions of species  $i$ . Of course,  $a_i \ll a$ , and the Einstein-Stokes diffusion coefficients  $D_i^\circ$  of the small ions are much larger than  $D^\circ = k_B T / \zeta^\circ$ .

The simplest approximate scheme is obtained if we describe the static properties  $\sigma_{ij}(\mathbf{r}, \mathbf{r}')$  and  $n_i^{\text{eq}}(r)$  within the Debye-Hückel approximation for the (point-like) electrolyte ions, and the "homogeneous fluid approximation" is adopted (see section 6). If, in addition, Fick's law is employed to describe the collective diffusion of the small ions,  $\Delta\zeta(t)$  may be evaluated explicitly [50]. Its long-time asymptotic result reads

$$\Delta\zeta(t) \approx \frac{Q^2}{6\pi\epsilon(D_s^\circ)^{3/2}} \frac{e^{-\kappa D_{\text{small}}^\circ t}}{t^{3/2}} \quad (t \rightarrow \infty) \quad (55)$$

where  $D_{\text{small}}^\circ$  is the Stokes-Einstein diffusion coefficient of the small ions. The time integral of  $\Delta\zeta(t)$  is  $\Delta\zeta^{\text{el}}$ , and the approximations just indicated lead to [49,51]

$$\Delta\zeta^{\text{el}} = \frac{Q^2 [1 - (1 + 2\kappa a)e^{-2\kappa a}]}{12\epsilon a D_{\text{small}}^\circ \kappa a}. \quad (56)$$

This happens to be the result previously derived by Schurr [48].

Once again, this derivation of a previously-available result illustrates the generality of the theory presented in section 6, and indicates several ways to extend its application to electrolyte friction. Thus, a simple expression for the time-dependence of  $\Delta\zeta(t)$ , which in principle could also be observed experimentally by light scattering techniques, is the first bonus of this approach. Furthermore, approximations such as the use of Debye-Hückel static correlations, the vanishing size of the small ions, and the homogeneous-fluid approximation, involved in Schurr's theory for  $\Delta\zeta^{\text{el}}$ , may also be avoided or replaced by less restrictive assumptions [51,52]. Unfortunately, the improvement of the theoretical results does not change the fact that electrolyte friction effects are generally small, and rather difficult to measure experimentally with high accuracy. Nevertheless, the theoretical relevance of this work lies on the fact that for the first time a single theoretical approach has provided a unifying view of this phenomenon and that of self-friction, both of which are present whenever we have charged colloidal particles in suspension.

Let us mention that in reality, it was to electrolyte friction where the method explained in section 6 was first applied [49] to derive a generalized Langevin equation of the form of Eq. (37). It was a further development [33] to notice that the same approach could also be used to describe the interaction of a tracer Brownian particle

with other diffusing macroparticles. As we saw in the previous sections, this has been a fruitful observation, and this is perhaps the main contribution of the pioneering attempt [47] to introduce the idea of contraction of the description to describe electrolyte friction.

## 9. Concluding remarks

As we have seen in this paper, a relatively simple picture is now available to describe, within the same theoretical scheme, three rather different aspects of the study of Brownian motion in colloidal suspensions. In the first place, we discussed the effects of macroparticle-macroparticle interactions, then we incorporated the effects of hydrodynamic interactions, and finally we applied the same ideas to the description of electrolyte friction. Traditionally, these three effects have been studied by rather different, and seemingly unrelated theoretical methods, and by somewhat disconnected communities. The advantage of having a general approach, besides its theoretical value, is that it allows the expansion of our understanding, to increasingly more complex systems and processes. For instance, the description of the static and dynamic properties of polydisperse suspensions (*i.e.*, with more than one type of colloidal species) is a relevant practical problem, posing a large number of basic questions. Although the first steps along the lines of the theories described in section 5 have been taken in this direction [27,53], concerning tracer-diffusion, still much is to be done to reach the same degree of qualitative and quantitative accuracy of the results compared and illustrated here for monodisperse suspensions. Concerning tracer-diffusion, it is likely that the multi-species extension in section 8 of the main results of the theory presented in section 6 will provide an accurate and convenient approach to the dynamics of polydisperse suspensions. As we saw in the previous section, such extension found already a neat application in the description of electrolyte-friction effects.

Another important practical problem is the description of self-diffusion of non spherical colloidal particles. Although suspensions of approximately spherical particles are no rare exception, for many systems and conditions the departure from such limiting case constitutes the main characteristic feature. This is so, for example, when we deal with biopolymeric materials such as DNA, with concentrated micellar solutions, or with magnetic colloids. With suspensions of non-spherical particles, progress has been slower, due to the understandable difficulties associated to the loss of a simplifying symmetry. We may say that the description of many dynamical properties of these systems encounter a severe difficulty in the non-availability of a practical description of the corresponding static quantities. However, this being a problem already considered in the physics of molecular fluids, one would expect that some of the advances in that field will be of assistance in the understanding of colloidal suspensions of non-spherical particles. After all, an analogy between simple liquids and suspensions of spherical colloidal particles was the basis for the progress in this field, as we have attempted to describe in this paper. One should also mention that one of the main features of the dynamics of non-spherical particles is the need



to describe rotational diffusion. Although in principle the method employed in the derivation of the main results in section 6 could also be extended to incorporate these effects, such an extension is not yet available. Let us mention, however, that the *translational* Brownian motion of non-spherical tracers in a bath of spherical macroparticles may be described by, essentially, the same general results of section 6. In fact, the first results of this type have recently been produced [52] in a simple extension of the results of the previous section for  $\Delta\zeta^{\text{el}}$ , to calculate the electrolyte friction on a charged spheroidal Brownian particle with a rather particular internal charge distribution. Although this is still a modest step in the understanding of the dynamics of non-spherical particles, it has provided preliminary indications [52] that electrolyte friction effects, which are small for spherical particles, may be more important for long rod-like tracers.

In summary, in this paper we have attempted to illustrate the power of the concepts and theories of fluctuations and Brownian motion, which originate from the classical work of Einstein, Langevin, Onsager, and others. This illustration was based on the description of tracer-diffusion phenomena in colloidal suspensions. As it happens, colloidal suspensions are a prominent class of complex fluids. Thus, we hope to have convinced the reader that at least when well-defined theoretical and experimental model systems are considered, the methods of physical research have converted a small piece of the land of complex fluids into a hospitable field of modern physics. Similar fronts in other aspects of the physics of complex fluids are being pursued, and one would expect that statistical physics will join the experimental physicist, chemist and materials scientist in the venture to render unjustified the "complex" portion of the name of these materials.

### Acknowledgements

The authors acknowledge R. Klein and G. Nägele for numerous discussions on many aspects of this work. We also thank CONACyT (Consejo Nacional de Ciencia y Tecnología) for economic support.

### References

1. V. Degiorgio and M. Corti, eds., *Physics of Amphiphiles: Micelles, Vesicles, and Microemulsions*. North Holland, Amsterdam (1985).
2. *Concentrated Colloidal Dispersions*. General Discussion No. 76. The Royal Society of Chemistry, Faraday Division (1983).
3. *Brownian Motion*. General Discussion No. 83. The Royal Society of Chemistry, Faraday Division (1987).
4. Les Houches School on Colloidal Crystals. Proceedings. *J. de Physique*, Colloque C3, Supplement au No. 3, Tome 46 (1985).
5. P.N. Pusey and R.J.A. Tough, Dynamic Light Scattering and Velocimetry, in: R. Pecora, ed. *Applications of Photon Correlation Spectroscopy*, Plenum, New York (1985).

6. A. Einstein, *Investigations of the theory of the Brownian movement*. Dover, New York (1956).
7. M. v. Smoluchowski, *Physik. Zeits.* **17** (1916) 557.
8. P. Langevin, *Comptes rendus* **146** (1908) 530.
9. W. Hess and R. Klein, *Adv. Phys.* **32** (1983) 173.
10. P. Mazur and W. van Saarloos, *Physica* **110A** (1982) 147.
11. G.K. Batchelor, *J. Fluid. Mech.* **74** (1976) 1.
12. J. Keizer, *Statistical Thermodynamics of Non-equilibrium Processes*. Springer-Verlag, New York (1987).
13. S.R. de Groot and P. Mazur, *Non-equilibrium Thermodynamics*. North Holland, Amsterdam (1962). Reprinted by Dover (1984).
14. J.P. Hansen and I.R. McDonald, *Theory of Simple Liquids*. Academic Press, New York (1976).
15. J. Hayter, *Faraday Discuss. Chem. Soc.* **76** (1983) 7.
16. E.J.W. Verwey and J.T.G. Overbeek, *Theory of the Stability of Lyophobic Colloids*. Elsevier, Amsterdam (1948).
17. M. Medina-Noyola and D.A. McQuarrie, *J. Chem. Phys.* **73** (1980) 6279.
18. R. Krause, G. Nägele, D. Karrer, J. Schneider, R. Klein, and R. Weber, *Physica* **153A** (1988) 400.
19. J.S. Hoye and L. Blum, *J. Stat. Phys.* **16** (1977) 399.
20. J.P. Hansen and J. Hayter, *Molec. Phys.* **46** (1982) 651.
21. (a) L. Cantú, M. Corti, and V. Gegiorgio, *Faraday Discuss. Chem. Soc.* **83** (1987) 287. (b) W.D. Dozier, Thesis, University of California, Los Angeles (1986).
22. B.J. Ackerson, *J. Chem. Phys.* **64** (1976) 242; **69** (1978) 684.
23. P.N. Pusey and R.J.A. Tough, *J. Phys. A: Math. Gen.* **15** (1982) 1291.
24. J.M. Deutch and I. Oppenheim, *J. Chem. Phys.* **54** (1971) 3547; T.J. Murphy and J.L. Aguirre, *J. Chem. Phys.* **57** (1972) 2098.
25. P. Mazur, *Physica* **110A** (1982) 128.
26. G. Nägele, M. Medina-Noyola, R. Klein, and J.L. Arauz-Lara, *Physica* **149A** (1988) 123.
27. J.L. Arauz-Lara, Thesis, Centro de Investigación y de Estudios Avanzados del IPN, Mexico City, 1985.
28. J.L. Arauz-Lara and M. Medina-Noyola, *Physica* **122A** (1983) 547.
29. J.L. Arauz-Lara and M. Medina-Noyola, *J. Phys. A: Math. Gen.* **19** (1986) L117.
30. J.L. Arauz-Lara and M. Medina-Noyola, *Kinam* **7** serie A, (1986) 135.
31. L. Onsager and S. Machlup, *Phys. Rev.* **91** (1953) 1505; **91** (1953) 1512.
32. M. Medina-Noyola and J.L. Del Rio-Correa, *Physica* **146A** (1987) 483.
33. Medina-Noyola, *Faraday Discuss. Chem. Soc.* **83** (1987) 21.
34. R.F. Fox and G.E. Uhlenbeck, *Phys. Fluids* **13** (1970) 1893; **13** (1970) 2881; E.H. Hauge and A. Martin-Löf, *J. Stat. Phys.* **7** (1973) 259; D.H. Berman, *J. Stat. Phys.* **20** (1979) 57.
35. B. Berne, *Statistical Mechanics, Part B: Time-dependent Processes*. B. Berne, ed. Plenum, New York (1977).
36. R. Evans, *Adv. Phys.* **28** (1979) 143.
37. W. van Megen, S.M. Underwood, R.H. Ottewill, N.S.J. Williams, and P. Pusey, *Faraday Discuss. Chem. Soc.* **83** (1987) 47.
38. A. van Veluwen, H.N.K. Lekkerkerker, C.G. de Kruijff, and A. Vrij, *Faraday Discuss. Chem. Soc.* **83** (1987) 59.
39. P. Mazur, *Faraday Discuss. Chem. Soc.* **83** (1987) 33.
40. B.U. Felderhof, *Physica* **89A** (1977) 373; *J. Phys. A: Math. Gen.* **11** (1978) 929.
41. C.W.J. Beenaker and P. Mazur, *Physica* **126A** (1984) 349.
42. P. Mazur and U. Geigenmuller, *Physica* **146A** (1987) 657.

43. M. Medina-Noyola, *Phys. Rev. Lett.* **60** (1988) 2705.
44. M. Medina-Noyola, *Lectures on Thermodynamics and Statistical Mechanics*, A. Gonzalez and C. Varea, eds. World Scientific, Singapore (1988).
45. G.A. Schumacher and Th.G.M. van de Ven, *Faraday Discuss. Chem. Soc.* **83** (1987) 75.
46. F. Booth, *J. Chem. Phys.* **22** (1954) 1956.
47. H. Ohshima, T.W. Healy and L.R. White, *J. Chem. Soc. Faraday Trans. 2*, **79** (1983) 1613.
48. J.M. Schurr, *Chem. Phys.* **45** (1980) 119.
49. M. Medina-Noyola and A. Vizcarra Rendón, *Phys. Rev. A* **32** (1985) 3596.
50. H. Ruiz-Estrada, A. Vizcarra-Rendón, M. Medina-Noyola, and R. Klein, *Phys. Rev. A* **34** (1986) 3446.
51. A. Vizcarra-Rendón, H. Ruiz-Estrada, M. Medina-Noyola, and R. Klein, *J. Chem. Phys.* **86** (1987) 2976.
52. A. Vizcarra-Rendón, Thesis, Centro de Investigación y de Estudios Avanzados del IPN, Mexico City (1989).
53. G. Nägele, M. Medina-Noyola, J.L. Arauz-Lara, and R. Klein, *Progr. Colloid and Polymer Sci.* **73** (1987) 5.

**Resumen.** Este trabajo revisa el estatus actual de la comprensión de los fenómenos de difusión de un trazador en suspensiones coloidales. Esta es la observación más directa del movimiento que ejecutan partículas brownianas marcadas que interactúan con el resto de las partículas coloidales en una suspensión. La descripción fundamental de este fenómeno constituye hoy en día uno de los problemas más relevantes en el proceso de comprender las propiedades dinámicas de esta importante clase de fluidos complejos, desde la perspectiva teórica y experimental de la investigación en física. Este trabajo describe los desarrollos recientes en la extensión de la teoría clásica del movimiento browniano y su aplicación en la descripción de los efectos de las interacciones directas e hidrodinámicas entre partículas coloidales. Como resultado se ha producido un marco coherente en el que el acuerdo entre teoría y experimento tiene el grado de precisión cualitativa y cuantitativa que se espera de campos de la física con mayor madurez. La moraleja es que el uso de conceptos bien establecidos de la física estadística, asistidos por técnicas experimentales modernas, está contribuyendo a transformar a los fluidos complejos en una clase más amigable de materiales, desde el punto de vista del físico.